Generation, transport, and preservation of the alkenone-based $U^{K'}_{37}$ sea surface temperature index in the water column and sediments of the Cariaco Basin (Venezuela)

Miguel A. Goni,[1] Mark P. Woodworth,[1] Heather L. Aceves,[1] Robert C. Thunell,[1] Eric Tappa,[1] David Black,[2] Frank Müller-Karger,[3] Yrene Astor,[4] and Ramon Varela[4]

Received 31 July 2003; revised 19 December 2003; accepted 30 January 2004; published 3 April 2004.

[1] Alkenone fluxes in the water column of the Cariaco Basin ranged from 12 to 20 μg m^{-2} d^{-1} and were inversely related to upwelling strength. The $U^{K'}_{37}$ ratios of sinking particles varied from 0.78 to 0.96 and exhibited seasonal changes that were coherent with a 7°C variation in sea surface temperature (SST). The correlation between SST and $U^{K'}_{37}$ ratios closely overlapped with the calibration of *Prahl et al.* [1988]. Alkenone burial fluxes in Cariaco Basin sediments varied markedly over the past ~6000 years, ranging from 0.2 to 5 μg m^{-2} d^{-1}. The $U^{K'}_{37}$ ratios of surface sediments indicate SST was higher (26.3°C) during the last 50 years of deposition than in the previous 300 years (~25°C), signaling an upwelling decrease in the latter part of the twentieth century. The lowest $U^{K'}_{37}$-derived temperatures (~25°C) were measured in sediments deposited during the little ice age (LIA). These compositions, coupled with relatively low alkenone fluxes (≤2 μg m^{-2} d^{-1}), are consistent with conditions of enhanced upwelling, decreased SST and reduced haptophyte production. The highest $U^{K'}_{37}$-derived SST estimates (over 26.5°C) were measured during the Medieval Warm Period (MWP) and suggest reduced upwelling at this time. Prior to the MWP, the alkenone record indicates temperatures of ~26°C and burial fluxes of ~2 μg m^{-2} d^{-1}. These compositions indicate stronger upwelling conditions during the Holocene relative to the last 50 years and the MWP but annual SSTs above those estimated for the LIA. *INDEX TERMS:* 1635 Global Change: Oceans (4203); 4267 Oceanography: General: Paleoceanography; 4279 Oceanography: General: Upwelling and convergences; 4850 Oceanography: Biological and Chemical: Organic marine chemistry; *KEYWORDS:* Alkenones, $U^{K'}_{37}$ Index, SST, Sediment Traps, Marine Sediments, Cariaco Basin, (10°30′N, 64°40′W)

Citation: Goni, M. A., M. P. Woodworth, H. L. Aceves, R. C. Thunell, E. Tappa, D. Black, F. Müller-Karger, Y. Astor, and R. Varela (2004), Generation, transport, and preservation of the alkenone-based $U^{K'}_{37}$ sea surface temperature index in the water column and sediments of the Cariaco Basin (Venezuela), *Global Biogeochem. Cycles*, *18*, GB2001, doi:10.1029/2003GB002132.

1. Introduction

[2] Long-chain alkenones, especially the tetra-, tri-, and di-unsaturated methyl C_{37} ketones, are some of the most widely utilized organic biomarkers in paleoceanographic investigations [*Eglinton et al.*, 2001]. It is well known that haptophyte algae, including the coccolithophores *Emiliania huxleyi* and *Gephyrocapsa oceanica*, synthesize these compounds and vary their degree of unsaturation in response to the water temperature in which they grow [*Marlowe et al.*, 1984; *Volkman et al.*, 1995, 1980]. Several laboratory culture experiments [*Conte et al.*, 1995, 1998; *Prahl et al.*, 1988; *Prahl and Wakeham*, 1987; *Volkman et al.*, 1995] have resulted in a variety of mathematical expressions that relate the extent of alkenone unsaturation, defined as the U^{K}_{37} or $U^{K'}_{37}$ ratio, to the growth temperature. In spite of significant differences in the temperature- $U^{K'}_{37}$ relationships obtained in cultures [*Herbert*, 2001; *Prahl et al.*, 2000b], several comprehensive "field calibration" efforts have shown that the $U^{K'}_{37}$ ratios of core top sediments and the average sea surface temperatures (SST) from many ocean regions are linearly correlated [*Herbert et al.*, 1998; *Müller et al.*, 1998; *Rosell-Melé et al.*, 1995b; *Sonzogni et al.*, 1997]. Notably, the field calibration relationships agree well with the widely utilized equation originally derived by *Prahl et al.* [1988].

[3] These findings have stimulated a large number of studies designed to reconstruct past SST conditions throughout the world's oceans based on the $U^{K'}_{37}$ ratios preserved in marine sediments (see recent reviews [*Bard*, 2001; *Mix et*

[1]Department of Geological Sciences, University of South Carolina, Columbia, South Carolina, USA.
[2]Department of Geology, University of Akron, Akron, Ohio, USA.
[3]Department of Marine Science, University of South Florida, St. Petersburg, Florida, USA.
[4]Estacion de Investigaciones Marinas de Margarita, Fundacion La Salle de Ciencias Naturales, Porlamar, Venezuela.

Copyright 2004 by the American Geophysical Union.
0886-6236/04/2003GB002132$12.00

al., 2000; *Sachs et al.*, 2000]). Such studies provide valuable information on past climate that is highly complementary to the results obtained from other paleotemperature proxies. Additional paleoceanographic applications of long chain alkenones include the use of their burial fluxes to reconstruct past phytoplankton productivity and assemblages [*Prahl et al.*, 1993, 2000a; *Villanueva et al.*, 1998; *Weaver et al.*, 1999; *Werne et al.*, 2000], as well as the use of their stable carbon isotopic compositions to estimate the levels of carbon dioxide in the surface ocean in order to reconstruct the partial pressure of CO_2 (pCO_2) in the atmosphere [*Jasper and Hayes*, 1990; *Jasper et al.*, 1994; *Pagani et al.*, 1999; *Popp et al.*, 1999].

[4] The alkenone-based reconstructions of past surface ocean conditions (temperature, productivity, pCO_2), however, are not without inherent problems [*Eglinton et al.*, 2001]. Among the important issues affecting the paleoceanographic applications of alkenones are those related to their generation in the euphotic zone, including the timing, location, and species responsible for the synthesis of these compounds (e.g., see reviews by *Volkman* [2000], *Bijma et al.* [2001], and *Pelejero and Calvo* [2003]). Most recently, nutrient and light stress have also been shown to affect the alkenone concentrations and compositions in cultured algae [*Conte et al.*, 1998; *Epstein et al.*, 2001; *Prahl et al.*, 2003]. In addition to these ecological, environmental, and physiological factors, the alteration of the primary signals (i.e., $\mathbf{U}^{\mathbf{K}'}_{\mathbf{37}}$ ratios, $\delta^{13}C_{alkenones}$) during alkenone transport through the water column and deposition and burial in sediments can lead to erroneous interpretations of compositions in the sedimentary record (see reviews by *Grimalt et al.* [2000] and *Harvey* [2000]).

[5] In this paper, we investigate how oceanographic and biologic processes (e.g., upwelling, water column stratification, primary productivity) in the euphotic zone control the production, export, and burial of long-chain alkenones in the water column and sediments from the Cariaco Basin off the Venezuelan coast. For this purpose, we analyzed sediment trap samples collected at three depths during a 3-year (1997–1999) period as part of the Carbon Retention in a Colored Ocean (CARIACO) time series study. Coupled with satellite-based observations and monthly cruises, which provided simultaneous observations of the sea surface and subsurface hydrography, these sediment trap samples represent an excellent opportunity to study the ecological and environmental factors affecting the paleoceanographic applications of alkenones. Specifically, in this study, we examine the production and temperature recording potential of alkenones in the context of seasonal water column temperature and biological productivity changes associated with three annual upwelling cycles. We also investigate the changes in alkenone fluxes and $\mathbf{U}^{\mathbf{K}'}_{\mathbf{37}}$ ratios that occur during particle settling through the water column of the Cariaco Basin in order to assess how the primary signals produced in the euphotic zone are transferred to the surface sediments. Additionally, we examine the concentrations and compositions of alkenones in sediments representing the last ~300 years of accumulation in the Cariaco Basin to assess the effects of sediment diagenesis on the $\mathbf{U}^{\mathbf{K}'}_{\mathbf{37}}$ ratios and reconstruct the recent history of upwelling at this site. Finally, we measure alkenone concentrations and compositions in sediments from a gravity core extending to ~6000 years before present to investigate the long-term trends in $\mathbf{U}^{\mathbf{K}'}_{\mathbf{37}}$ ratios and what they can tell us about the SST history of the Cariaco Basin during the middle to late Holocene.

2. Samples and Methods

[6] All of the samples presented in this paper were collected from the eastern sub-basin of the Cariaco Basin (Figure 1), a 1400-m-deep depression on the continental shelf off the Venezuelan central coast. The basin is connected with the surface Atlantic Ocean above a shallow (100 m) sill, which is breached by two channels (the Canal de la Tortuga and the Canal Centinela). Because of its location within the shelf and its restricted water circulation, the Cariaco Basin acts as natural sediment trap [*Lidz et al.*, 1969; *Richards*, 1975] and displays permanent anoxic conditions below ~275 m [*Deuser*, 1973]. The sediments underlying the Cariaco Basin contain extensively varved sections and display relatively high accumulation rates. As such, they represent an exceptional archive that has been the focus of numerous paleoceanographic and paleoclimatic investigations [*Black et al.*, 1999, 2001; *Haug et al.*, 1998; *Hughen et al.*, 2000, 1996; *Overpeck et al.*, 1989; *Peterson et al.*, 1991; *Werne et al.*, 2000].

[7] In November of 1995, the CARIACO time series was started with the goal of conducting a systematic study of the carbon cycle in the Cariaco Basin. The program is composed of investigators from several U.S. and Venezuelan institutions and includes monthly measurements of basic hydrographic properties and primary productivity, as well as chemical analyses of the water column at the CARIACO station (Figure 1). In addition, sediment traps have been in place since the start of the project, collecting sinking particles from the water column at bi-weekly intervals. Satellite observations provide continual data on the conditions in the surface ocean. An overview of the extent of activities of the program is available at the CARIACO web site (http://imars.marine.usf.edu), which also serves as a data repository. Most of the methods utilized for the acquisition and analyses of samples presented in this paper have been described in detailed in previous publications [*Astor et al.*, 2003; *Goni et al.*, 2003; *Müller-Karger et al.*, 2001; *Scranton et al.*, 2001; *Taylor et al.*, 2001; *Thunell et al.*, 2000]. A brief description of each of them is provided below.

2.1. Water Column Measurements

[8] SST data were obtained from imagery collected with the advanced very high resolution radiometer (AVHRR) sensors on the NOAA 11, 12, and 14 satellites using the split window techniques as described by *Müller-Karger et al.* [2001]. Monthly cruises to the time series site (10°30′N, 64°40′W) were conducted during the study period (November 1996 to October 1999) using the Buque Oceanográfico Hermano Ginés, operated by Fundación La Salle de Ciencias Naturales (FLASA) from the Estación de Investigaciones Marinas Margarita (EDIMAR) located on Isla Margarita. A

Figure 1. Map of the Cariaco Basin. The locations of the CARIACO station, where monthly cruises take place and the sediment trap is located, and the sites where the multicore (MC-4) and the gravity core (CAR7-2) were taken are indicated.

rosette-mounted Seabird™ CTD was used to obtain continuous profiles of conductivity and temperature at 1-m resolution for the top 100 m of the water column. Water samples were collected at eight depth intervals (1–2, 6–8, 14–16, 24–26, 34–36, 54–56, 74–76, and 98–100 m). Among the various biogeochemical measurements made on the samples collected each month, chlorophyll-a concentrations were measured in particles isolated by filtration (25-mm GF/F filters) of 250 to 500 mL of water. Filters were extracted in methanol and chlorophyll-a concentrations determined on a Turner Designs fluorometer using standard methods [*Falkowski and Kiefer*, 1985; *Holm-Hansen et al.*, 1965].

2.2. Sediment Trap Collection

[9] A single mooring containing four automated sediment traps [*Honjo and Doherty*, 1988] was deployed in the eastern sub-basin of the Cariaco Basin (10°30′N, 64°40′W) at a depth of approximately 1400 m (Figure 1) as described by *Thunell et al.* [2000]. Each cone-shaped trap has a 0.5 m^2 collection area that is covered with a baffle to reduce turbulence over the trap. The traps were placed at four different depths: Trap A at 275 m, just above the oxic/anoxic interface, Trap B at 455 m, Trap C at 930 m and Trap D at 1255 m. Each trap contains a 13-cup carousel that was programmed to collect samples at 2-week intervals, and the mooring was deployed over a 6-month period. A buffered formalin solution was placed in each trap cup prior to deployment in order to minimize post-depositional degradation of the organic matter. After collection, samples were stored in sealed containers and kept refrigerated until analyses. Prior to analyses, samples were thoroughly washed with distilled water to remove excess formalin and carefully examined under the microscope to remove swimmers that are not part of the particle flux [*Thunell et al.*, 2000]. Samples were dried in either an oven (50°C) or a freeze drier and weighed to obtain the total mass flux (g m^{-2} d^{-1}).

2.3. Sediment Collection

[10] Sediments were collected from a relatively flat portion of the north side of the eastern basin (Silla de Araya; Figure 1), which minimized the occurrence of turbidites. In November 1998, we used a gravity corer to collect a 220-cm-long core (CAR7-2) from the Silla de Araya (10°39.055′N, 64°39.595′W, 449 m water depth). Once collected, the gravity core was kept upright and covered, while the top was allowed to air-dry and consolidate for 48 hours. The core was split lengthwise, one half of the core was subsampled at 0.5-cm intervals throughout its length, and selected horizons were used for geochemical analyses. The sediments were stored in sealed K-Pack bags and kept frozen until analyses. The other half of the core was subsampled at consecutive millimeter intervals of known volume over its entire length. These samples were dried, weighed, and used to construct an age model [*Black et al.*, 2001] based on the dry bulk density data and accelerator mass-spectrometry (AMS) ^{14}C dates of isolated samples of the planktic foraminifer *Globigerina bulloides* [*Goni et al.*, 2003].

[11] On November 1, 2000, we used an Ocean Instruments MultiCorer to retrieve a 47-cm-long core (MC-4) with an intact sediment-water interface from approximately the same location (10°38.98′N, 64°39.64′W, 432 m water depth). After collection, the core was sliced on the ship at 0.5-cm intervals for the top 10 cm and at 1-cm intervals through the rest of the core. Sediment samples were sealed in K-Pack bags and kept frozen during transport to the laboratory and stored frozen until analysis. Subsamples from each horizon were placed in pre-weighed vials of known volume to determine water content and porosity.

2.4. Organic Carbon Analyses

[12] Weight percent organic carbon (%OC) content was determined in all samples after acidification to remove carbonates using the procedures described by *Goni et al.* [2000, 2001]. Following acidification, samples were combusted at high temperature (1000°C) and the amounts of the resulting CO_2 measured using a either a Perkin-Elmer 2400 or a ThermoQuest 2500 EA. The response of the EA detectors were determined daily through standard calibrations of cystine standards. The average error of %OC determination was 2% of the measured value.

2.5. Alkenone Analyses

[13] The concentrations of the two major long-chain alkenones, di- and tri-unsaturated methyl C_{37} ketones ($C_{37:2}$ and $C_{37:3}$, respectively), were determined using a slightly modified procedure developed by *Rosell-Melé et al.* [1995a] as described by *Goni et al.* [2001]. Briefly, known amounts of dried ground sample were extracted using sonication in triplicate with a 3:1 dichloromethane/methanol solution using a Benchmate™ II Workstation. Prior to the extraction step, hexatriacontane was added as a recovery standard. The initial extracts were cleaned using preconditioned solid phase extraction columns and eluted using a solution of dichloromethane with 1% methanol. Prior to gas chromatographic (GC) analyses, the extracts were silylated with Regisil (BSTFA + 1%TCMS; Regis Technologies, Inc.) overnight, dried, and redissolved in dichloromethane. GC analyses were carried out on a Hewlett-Packard 6890 GC equipped with on-column injector and flame ionization detector (FID). We used a 60-m DB-1 GC column with 0.32-mm internal diameter and 0.25-μm film thickness. The concentrations of the long-chain alkenones were determined assuming the same FID response factor as the hexatriacontane standard. The identities of the individual alkenones and hexatriacontane were confirmed by co-injection of synthetic standards and by mass spectrometric analyses using a Varian 2000 Saturn ion trap GC-MS. The alkenones unsaturation index, i.e., $\mathbf{U}^{\mathbf{K}'}_{37}$ ratio, was calculated based on the concentration of the $C_{37:2}$ and $C_{37:3}$ methyl ketones according to *Prahl and Wakeham* [1987],

$$\mathbf{U}^{\mathbf{K}'}_{37} = [C_{37:2}]/[C_{37:2} + C_{37:3}]. \quad (1)$$

[14] The average error associated with the determination of alkenones concentrations was 10–30% of the measured value, with the larger variability being associated with those samples with lowest concentrations. The average variability associated with the $\mathbf{U}^{\mathbf{K}'}_{37}$ ratio determination was 0.01, which corresponds to an analytical error of 0.3°C in the determination of the alkenone-based temperature.

3. Results

3.1. Hydrographic Trends

[15] The surface waters in the Cariaco Basin undergo a marked seasonal cycle of upwelling and stratification driven by changes in trade wind intensity associated with the seasonal migration of the intertropical conversion zone (ITCZ) [*Herrera and Febres-Ortega*, 1975]. These changes assert a primary control in the productivity and biogeochemistry of the Cariaco Basin [*Astor et al.*, 2003; *Goni et al.*, 2003; *Müller-Karger et al.*, 2001; *Scranton et al.*, 2001; *Taylor et al.*, 2001; *Thunell et al.*, 2000; *Walsh et al.*, 1999]. Most importantly for the focus of this paper, the annual upwelling-stratification cycle results in strong contrasts in SST. For example, from 1993 to 2001, daily SST values ranged from as low as 20°C at the peak of upwelling in winter months to as high as 29°C at maximum stratification during late summer and early fall (Figure 2). The main upwelling period normally started in November or December and lasted several months until March or April. Typically, a short secondary upwelling event occurred during the late spring and early summer (May/June) of each year. The timing and extent of the sea surface seasonal cooling during maximum upwelling varied significantly depending on the year, with minimum monthly average temperatures that ranged from 22° to 23°C (Figure 2). The onset of thermal stratification typically started during the summer months and peaked in the late fall (September/October). Marked contrasts in the maximum monthly SST estimates were obvious in the 8-year AVHRR record (Figure 2), with values ranging between 25° to 28.5°C. In a typical year, SST in the Cariaco Basin underwent ~5°C change over a period of 6 months.

[16] The monthly hydrocasts between November 1996 and October of 1999 period, which is the focus of this study, showed that the temperature changes in the euphotic zone (Figure 3a) were consistent with SST variations and agreed with previously discussed trends [*Astor et al.*, 2003, and references therein]. Marked annual contrasts in the intensity and duration of the upwelling-stratification regimes were evident among the three years examined in this study (Figure 3a). The 1996–1997 upwelling period was the most intense and extensive (Figure 3a), leading to a marked decrease in water temperatures, with the 22°C isotherm shoaling to 10 m water during the height of the upwelling (February–March 1997). The secondary upwelling event this year was also intense, with the 22°C isotherm shoaling to the 20-m mark in July/August, 1997. In contrast, upwelling was more subdued in the two following years, with the 22°C isotherm barely reaching 25 m in March 1998 and only shoaling to 30 m in February 1999. During the 1997–1998 upwelling period we measured the rapid warming and thermal stratification of the upper water column from December 1997 to February of 1998 (Figure 3a). This trend was caused by the lateral intrusion of a massive anticyclonic eddy (680 × 300 km) from the Caribbean [*Astor et al.*, 2003; *Scranton et al.*, 2001] that temporarily suppressed

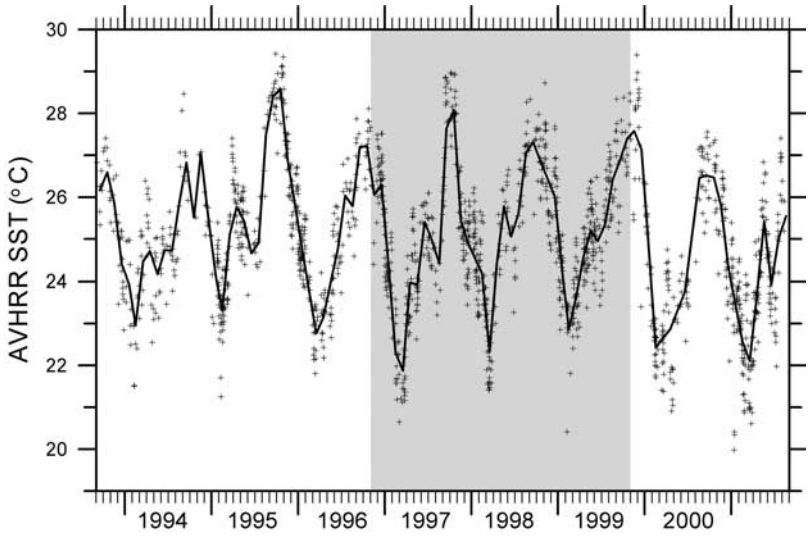

Figure 2. Sea surface temperature (SST) record derived from advanced very high resolution radiometer (AVHRR) satellite sensors. Individual data (pluses) as well as the monthly means (solid line) are plotted. The shaded box highlights the period which is the focus of this study.

upwelling and facilitated the warming of the surface ocean during this period (Figures 2 and 3a). Upwelling resumed in February and March 1998, during which two relatively large sized cyclonic eddies passed through the area [*Astor et al.*, 2003].

[17] In all 3 years, intense heating and thermal stratification of the surface ocean was observed in the late summer and fall (Figure 3). The shutdown of upwelling coincided with the seasonal decrease in trade Wind velocities and the northward migration of the ITCZ [*Astor et al.*, 2003]. Under these conditions, daily SST readings often exceeded 28°C and the water column underwent significant warming, with the 25°C isotherm often reaching depths greater than 30 m for prolonged periods. Thermal stratification was most intense during 1999, which was characterized by the lack of a marked secondary upwelling event during this year resulting in prolonged warming of the sea surface over much of that year.

[18] Elevated chlorophyll concentrations were consistently measured in surface waters during periods of strong upwelling (Figure 3b). In fact, most of the chlorophyll standing stock was concentrated in the top 25 m of the water column throughout most of the 3-year study. Subsurface chlorophyll maxima were evident during the periods of stratification in the summer and early fall in 1998 and especially 1999. Primary production rates were also always highest in the 25 m of the water column and displayed an overall similar distribution to that of chlorophyll concentrations [*Goni et al.*, 2003]. These observations indicate that most of the annual phytoplankton productivity during the study period originated from the surface waters (0–25 m) and was supported by the entrainment of nutrient-rich waters during upwelling [*Goni et al.*, 2003]. Notably, subsurface production was only important during periods of thermal stratification when export fluxes were low [*Goni et al.*, 2003]. Table 1 summarizes the temperature and chlorophyll data collected during the monthly cruises from the surface waters in Cariaco Basin. The table includes the depth-integrated temperature over the top 25 m of the water column (T_{0-25m}) as a useful parameter that has been previously applied to differentiate upwelling ($T_{0-25m} < 24.5$°C) versus non-upwelling conditions ($T_{0-25m} > 24.5$°C) [*Goni et al.*, 2003].

[19] Because the monthly cruises only provided snapshots of the temperature regime in the Cariaco Basin, it was difficult to assess directly the effect of upwelling on the composition of the sinking particles collected over 2-week intervals, especially when the temperature in the euphotic zone underwent rapid changes (Figure 3). The AVHRR data have the potential to overcome the temporal differences in coverage between the monthly cruises and the sediment traps by providing a semi-continuous record of SST conditions at the study site. A strong correlation was evident between the AVHRR SST data and T_{0-25m}, (Figure 4), indicating that the AVHRR SST data provide a reasonable measure of the temperature regime in the surface ocean. Thus we can use the daily AVHRR SST to reconstruct the mean temperature of the top of the euphotic during each of the sediment trap collection periods. We used these estimates to test the reliability of the alkenone-based $\mathbf{U}^{\mathbf{K}'}_{\mathbf{37}}$ SST index measured in sediment trap samples (see following discussion).

[20] In order to fully describe the hydrography of the Cariaco Basin, one has to consider the effects of the anticyclonic and cyclonic eddies that periodically pass through the area every few months. Besides the putative effect on SST (and on $\mathbf{U}^{\mathbf{K}'}_{\mathbf{37}}$ signatures), these eddies are responsible for the lateral intrusions of water masses into the interior of the basin, which result in the input oxygenated waters from the Caribbean Sea [*Astor et al.*, 2003]. Such features cause a temporary deepening of the oxycline and an enhancement of microbial activity in that region of the water column [*Taylor et al.*, 2001; *Scranton et al.*, 2001]. In some cases, enhanced phytoplankton productivities are also observed following the passage of eddies [*Astor et al.*,

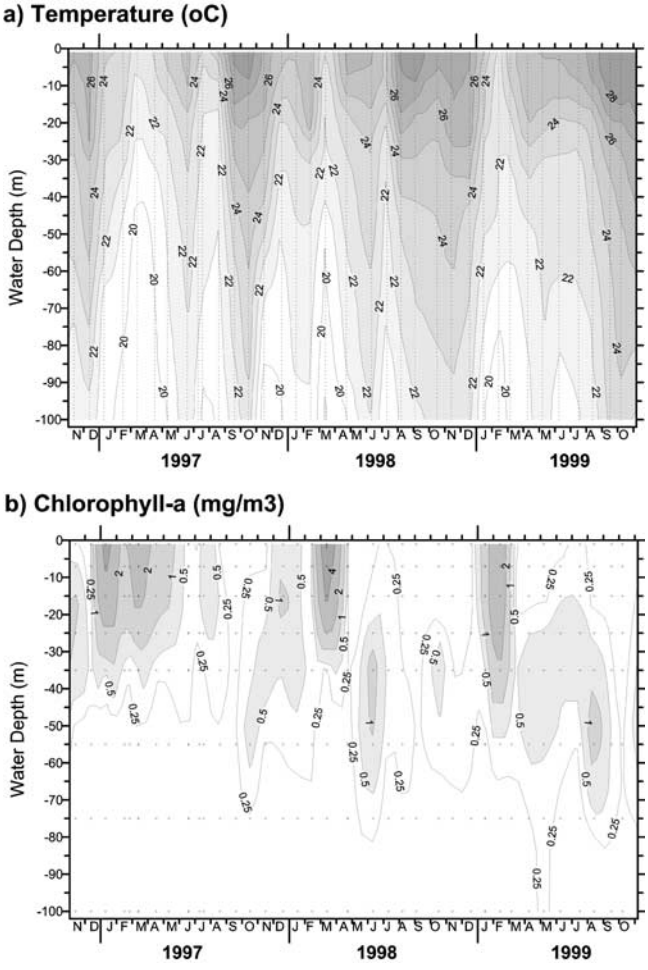

Figure 3. Profiles of (a) temperature (°C) and (b) chlorophyll-a concentration (mg m^{-3}) of the top 100 m of the water column in the Cariaco Basin collected during monthly cruises to the study site (Figure 1). Temperature measurements were done continuously using the CTD, while chlorophyll-a concentrations were measured from individual water samples collected at specific depths. The locations of the measurements are indicated in each graph.

2003]. Notably, these lateral intrusions are accompanied by elevated current velocities, which increase the potential for undertrapping sinking particles by sediment traps [*Goni et al.*, 2003] and the entrainment of allocthonous materials into the basin. Besides the aforementioned eddies observed over the Cariaco Basin in December 1997 (anticyclone) and February and March 1998 (cyclones), other significant lateral intrusions were observed in January 1997 (anticyclone), June and August 1997 (cyclones), June 1998 (anticyclone), and August 1998 (cyclone) [*Astor et al.*, 2003]. The effects of some of these events on alkenone fluxes and the $\mathbf{U}^{K'}_{37}$ index of sinking particles will be considered in the discussion below.

3.2. Alkenone Compositions in Sinking Particles

[21] The concentrations of the two major individual alkenones, $C_{37:2}$ and $C_{37:3}$, measured in sinking materials collected over the 3-year study period of this study (November 1996 to October 1999) are presented in Table 2. Consistently, $C_{37:2}$ was the most abundant alkenone in all samples analyzed with concentrations that ranged from 5 to 80 μg/g sample and showed considerable seasonal and depth variability. In contrast, $C_{37:3}$ was much less abundant, ranging from 0.3 to 18 μg/g and accounting for ~6 to 20% of $C_{37:2}$ yields. The tetra-unsaturated compound, $C_{37:4}$, was not detected in any of the samples collected. Also included in this table are estimates of the mean SST for the duration of each trapping period derived from the AVHRR data, the total mass flux collected in each cup, and the organic carbon content of each sample for which alkenone measurements were made. Trends in the composition and fluxes of biogenic materials including organic carbon, opal, calcium carbonate, and total alkenones have been discussed previously [*Goni et*

Table 1. Hydrographic Data November 1996 to October 1999[a]

Day, 1 Nov. 1995 = Day 1	Date of Cast	Average Temperature 0–25 m, °C	Cumulative Chlorophyll 0–100 m, mgChl/m^2
376	10 Nov. 1996	25.4	56.8
406	09 Dec. 1996	26.3	17.9
434	07 Jan. 1997	23.7	126.3
471	13 Feb. 1997	23.5	39.0
498	12 March 1997	21.5	82.6
532	15 April 1997	22.6	43.0
557	10 May 1997	23.2	42.9
595	17 June 1997	24.6	24.3
616	08 July 1997	23.3	16.7
624	16 July 1997	22.6	37.4
656	17 Aug. 1997	23.0	26.0
687	17 Sept. 1997	27.3	12.4
714	14 Oct. 1997	27.3	36.3
376–714	Nov. 1996 to Oct. 1997 averages	24.3	44.5
744	13 Nov. 1997	26.2	25.1
778	17 Dec. 1997	23.8	45.7
806	14 Jan. 1998	24.3	43.5
834	11 Feb. 1998	25.2	32.0
863	12 March 1998	22.2	126.2
903	21 April 1998	25.0	13.3
952	09 June 1998	25.0	59.9
982	09 July 1998	23.9	22.3
1009	05 Aug. 1998	27.4	24.2
1036	01 Sept. 1998	27.2	15.0
1079	14 Oct. 1998	26.2	25.9
744–1079	Nov. 1997 to Oct. 1998 averages	25.1	39.4
1106	10 Nov. 1998	27.0	19.1
1142	16 Dec. 1998	26.8	24.0
1169	12 Jan. 1999	24.1	46.9
1198	10 Feb. 1999	22.3	142.3
1220	04 March 1999	23.6	35.8
1254	07 April 1999	25.4	38.6
1283	06 May 1999	25.1	44.7
1315	08 June 1999	25.0	34.5
1353	15 July 1999	25.2	33.8
1380	11 Aug. 1999	25.5	57.1
1414	14 Sept. 1999	28.0	-
1435	05 Oct. 1999	27.7	11.9
1106–1435	Nov. 1998 to Oct. 1999 averages	25.5	44.4

[a]All data calculated from the monthly hydrocast measurements. Average Temperature 0–25 m represents the average temperature for the top 25 m of the water column. Cumulative Chlorophyll 0–100 m represents the cumulative chlorophyll concentrations of the top 100 m of the water column.

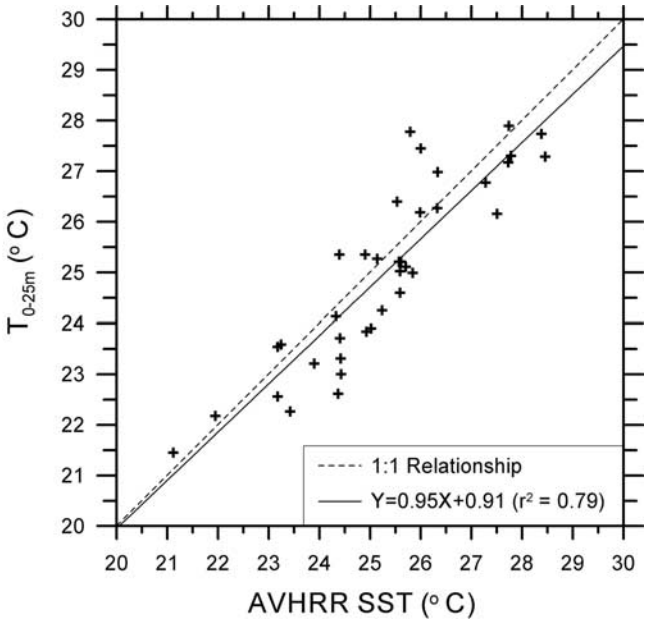

Figure 4. Correlation between satellite-derived sea surface temperatures (AVHRR SST) and the average temperatures for the top 25 m of the water column (T_{0-25m}) collected by CTD during the monthly cruises. For this correlation, we selected AVHRR SST data taken within 36 hours of when the CTD measurements were made. In cases when more than one AVHRR SST observation was made, we used the average value of all data available for the 36-hour period.

al., 2003]. In this paper we focus on the timing and magnitude of the flux of individual alkenones and the factors controlling the generation and transport of the $\mathbf{U}^{\mathbf{K'}}_{\mathbf{37}}$ temperature index in the water column of the Cariaco Basin.

[22] The total alkenone/organic carbon ratios (ΣAlk_{37}/OC) of particles exported from the euphotic zone (trap A samples) ranged from 0.1 to 0.6 mg/g and showed a poor overall correlation with SST (Figure 5). Nevertheless, ΣAlk_{37}/OC ratios were generally low (0.1 to 0.3 mg/g) during upwelling periods whereas during non-upwelling periods the ratios were much more variable and included the highest values observed during the 3-year period. In the first half of 1997, the samples from traps B and C followed the same trends as those from trap A. However, beginning in August 1997, we measured elevated ΣAlk_{37}/OC ratios (0.4 to 0.9) in samples from traps B and C. It appears that with the exception of the intense upwelling period in January–May 1997, alkenones were transported through the water column more efficiently than bulk OC [*Goni et al.*, 2003]. The water column fluxes of OC and ΣAlk_{37} during each of the three upwelling-stratification cycles are illustrated in Figure 6. The fluxes of these materials as a function of depth (F_z) were fitted to an exponential decay function [*Christian et al.*, 1997],

$$F_z = F_{150} e^{k(z-150)}, \quad (2)$$

where F_{150} is the estimated mean flux at 150 m and k represents the loss rate constant (m^{-1}) as particles sink.

[23] Evidence for the reduced lability of alkenones relative to OC during vertical transport thought the water column can be seen in the contrasts of reactivity rates determined using this approach (Figure 6). The loss rate constants for ΣAlk_{37} (average k = -0.0002 m^{-1} ± 0.0001) were 5 times smaller than those estimated for OC (average k = -0.001 m^{-1} ± 0.001). The differences in reactivity meant that on average, over 50% of the OC flux measured in trap A at 250 m disappeared by the time sinking particles reached trap C at 930 m (Figure 6). In contrast, less than 35% of the alkenone flux was lost between traps A and C in most years, with the losses during 1997–1998 being the least pronounced. Assuming an average sinking rate of 100 m d^{-1}, the estimated average degradation rate constant for ΣAlk_{37} during their transport through the water column was -0.02 d^{-1} (i.e., k ≈ -7.3 yr^{-1}), whereas the water column degradation rates for OC were ∼-0.1 d^{-1} (i.e., k ≈ -36.5 yr^{-1}). Using the same approach to estimate the decay constants for the individual alkenones (data not shown), we calculated comparable values for both the $C_{37:2}$ and $C_{37:3}$ compounds (average k values of -0.00022 m^{-1} ± 0.00017 and -0.00016 m^{-1} ± 0.00016, respectively).

3.3. Alkenone Compositions in Surface Sediments

[24] The organic carbon and alkenone concentrations of the sediments recovered from MC-4 are presented in Table 3. The ages of the sedimentary horizons were determined using the sedimentation rates determined by *Black* [1998], which averaged 0.11 ± 0.047 cm yr^{-1} in this region of the Cariaco Basin. The water content measurements of specific sediment samples were consistent with steady state compaction [*Berner*, 1980] and were fitted to estimate the distribution profile of porosity (p) with depth (z) according to

$$p = 0.0849 \times e^{(-0.0554z)} + 0.85 \left(r^2 = 0.88\right). \quad (3)$$

By assuming that pore water salinity was similar to the bottom water salinity at the time of collection (S = 36.32 ppt), we were able to plot the %OC and ΣAlk_{37} contents versus the age of sediments on a salt-free dry weight (SFDW) basis (Figure 7).

[25] Sedimentary organic carbon content ranged from 5 to 7% SFDW, and remained rather constant throughout the core (Figure 7a). In contrast, ΣAlk_{37} concentrations were highest near the sediment water interface (∼7 μg/g SFDW) and decreased significantly over the last 100 years of deposition to values of ∼2 μg/g SFDW (Figure 7b). The ΣAlk_{37} concentrations remained relatively unchanged in the sediments deposited between 100 and 250 ybp, ranging between 2 and 3 μg/g SFDW. The only exceptions were the elevated values (4 μg/g SFDW) measured in sediments deposited ∼200 ybp and the relatively low concentrations (<2 μg/g SFDW) measured in sediments older than 280 ybp. The ΣAlk_{37}/OC ratios of MC-4 samples ranged from 0.1 to 0.02 (Figure 7c). The ΣAlk_{37}/OC ratios decreased markedly over the upper portion of the core, reaching values of 0.025 in sediments deposited ∼80 ybp. The ΣAlk_{37}/OC ratios remained rather constant in the rest of the sediments, ranging from 0.03 to 0.05. The 200 ybp sample yielded relatively elevated ΣAlk_{37}/OC ratios of 0.06, while ratios decreased to <0.02 in the bottom horizons of the core (Figure 7c).

Table 2. Sediment Trap Data for Deployment Periods in Which Alkenone Measurements Were Made[a]

Deployment Code/Description	Cup Open	Cup Close	Mid-Day (11/1/95 = 1)	Duration, days	VHRR DATA Avg. SST, °C	VHRR DATA S.D. SST, °C	n
			Nov. 1996 to Oct. 1997				
car3-01	11/08/96	11/22/96	381	14	24.6	0.4	2
car3-03	12/06/96	12/20/96	409	14	26.7	0.4	20
car3-05	01/03/97	01/17/97	437	14	24.2	0.4	15
car3-07	01/31/97	02/14/97	465	14	23.1	0.4	4
car3-08	02/14/97	02/28/97	479	14	22.1	0.6	14
car3-09	02/28/97	03/14/97	493	14	21.2	0.5	4
car3-10	03/14/97	03/28/97	507	14	21.7	0.4	14
car4-01	05/15/97	05/22/97	562	7	23.8	0.3	9
car4-03	06/05/97	06/19/97	590	14	25.4	0.4	7
car4-05	07/03/97	07/17/97	618	14	24.7	0.4	9
car4-07	07/31/97	08/14/97	646	14	23.9	0.6	5
car4-09	08/28/97	09/11/97	674	14	26.6	1.2	12
car4-11	09/25/97	10/09/97	702	14	28.1	0.7	8
car4-13	10/23/97	11/13/97	727	11	27.0	1.1	13
Nov. 1996 to Oct. 1997 averages					**24.5**	**2.1**	
			Nov. 1997 to Oct. 1998				
car5-01	11/13/97	11/20/97	744	7	25.7	0.5	8
car5-03	12/04/97	12/18/97	772	14	24.6	0.6	20
car5-05	01/01/98	01/15/98	800	14	25.4	0.4	17
car5-07	01/29/98	02/12/98	828	14	24.4	0.8	15
car5-09	02/26/98	03/12/98	856	14	22.7	0.8	17
car5-11	03/26/98	04/09/98	884	14	23.5	0.5	4
car5-13	04/23/98	05/03/98	909	11	24.8	0.5	7
car6-01	06/03/98	06/10/98	946	7	25.9	1.1	2
car6-03	06/17/98	06/24/98	960	7	25.3	0.0	2
car6-05	07/01/98	07/15/98	981	14	24.6	0.6	5
car6-06	07/15/98	07/29/98	995	14	26.2	0.5	8
car6-07	07/29/98	08/12/98	1009	14	26.3	0.7	6
car6-09	08/26/98	09/09/98	1037	14	27.6	0.7	3
car6-11	09/23/98	10/07/98	1065	14	27.3	0.5	5
car6-13	10/21/98	11/02/98	1091	12	26.7	0.3	7
Nov. 1997 to Oct. 1998 averages					**25.4**	**1.4**	
			Nov. 1998 to Oct. 1999				
car7-01	11/07/98	11/19/98	1110	14	26.3	0.8	14
car7-02	11/21/98	12/03/98	1124	14	25.4	0.6	8
car7-03	12/05/98	12/17/98	1138	14	26.7	0.7	10
car7-05	01/02/99	01/14/99	1166	14	24.2	0.6	20
car7-07	01/30/99	02/11/99	1194	14	22.8	0.9	9
car7-09	02/27/99	03/11/99	1222	14	23.4	0.5	15
car7-11	03/27/99	04/08/99	1250	14	22.9	n.d.	1
car7-12	04/10/99	04/22/99	1264	14	24.7	0.4	18
car8-01	05/06/99	05/18/99	1290	14	25.5	0.6	16
car8-02	05/20/99	06/01/99	1304	14	25.1	0.5	18
car8-03	06/03/99	06/15/99	1318	14	25.1	0.8	10
car8-04	06/17/99	06/29/99	1332	14	24.5	0.7	7
car8-05	07/01/99	07/13/99	1346	14	24.8	0.8	7
car8-07	07/29/99	08/10/99	1374	14	26.3	0.7	16
car8-08	08/12/99	08/24/99	1388	14	26.2	0.6	6
car8-10	09/09/99	09/21/99	1416	14	26.2	1.1	5
car8-12	10/07/99	10/19/99	1444	14	26.9	0.4	7
Nov. 1998 to Oct. 1999 averages					**25.1**	**1.3**	

Deployment Code/Description	Total Mass Flux, $g/m^2/d$ Trap A (275 m)	Trap B (455 m)	Trap C (930 m)	%OC, g/100 g Trap A (275 m)	Trap B (455 m)	Trap C (930 m)
			Nov. 1996 to Oct. 1997			
car3-01	0.509	0.357	0.246	7.8	8.6	9.5
car3-03	0.346	0.225	0.207	7.3	7.7	8.2
car3-05	0.403	0.379	0.307	11.3	10.1	11.9

Table 2. (continued)

Deployment Code/Description	Total Mass Flux, g/m^2/d			%OC, g/100 g		
	Trap A (275 m)	Trap B (455 m)	Trap C (930 m)	Trap A (275 m)	Trap B (455 m)	Trap C (930 m)
car3-07	0.234	0.129	0.102	12.9	14.5	14.1
car3-08	0.779	0.384	0.276	11.4	12.1	13.6
car3-09	0.757	0.498	0.284	12.5	13.4	15.0
car3-10	0.875	0.453	0.712	14.1	14.2	17.7
car4-01	1.030	0.632	0.642	11.5	11.3	10.0
car4-03	1.056	0.149	0.189	7.7	6.3	8.4
car4-05	0.965	0.167	0.168	7.5	13.2	11.8
car4-07	1.137	0.482	0.162	7.5	8.8	12.6
car4-09	0.563	0.119	0.070	7.4	10.8	14.5
car4-11	0.602	0.079	0.022	5.8	7.4	9.7
car4-13	0.480	0.085	0.047	4.5	6.7	8.3
Nov. 1996 to Oct. 1997 averages	**0.695**	**0.296**	**0.245**	**9.2**	**10.4**	**11.8**
			Nov. 1997 to Oct. 1998			
car5-01	0.735	0.565	0.371	9.5	6.8	6.9
car5-03	1.013	1.019	0.731	11.0	9.0	8.7
car5-05	0.582	0.671	0.558	11.8	11.3	10.4
car5-07	0.187	0.505	0.279	14.3	13.7	13.6
car5-09	0.805	0.139	0.109	6.2	11.8	12.0
car5-11	1.537	0.435	0.451	9.4	17.2	17.0
car5-13	0.628	0.157	0.108	7.2	11.2	13.9
car6-01	0.672	0.286	0.255	9.6	9.9	9.8
car6-03	1.072	0.643	0.574	7.7	8.1	8.7
car6-05	0.489	0.279	0.181	11.6	9.9	11.7
car6-06	0.469	0.591	0.333	17.3	12.8	15.3
car6-07	0.661	0.473	0.215	6.6	6.1	9.0
car6-09	1.131	0.497	0.297	5.7	6.6	7.5
car6-11	1.048	0.295	0.154	7.8	12.7	15.8
car6-13	0.559	0.041	0.021	5.5	6.4	
Nov. 1997 to Oct. 1998 averages	**0.773**	**0.440**	**0.309**	**9.4**	**10.2**	**11.5**
			Nov. 1998 to Oct. 1999			
car7-01	0.690	0.404	0.445	8.0	6.9	6.5
car7-02	0.902	0.477	0.361	7.5	7.5	7.2
car7-03	0.735	0.677	0.557	6.3	6.4	6.8
car7-05	0.143	0.135	0.111	12.6	12.6	10.8
car7-07	0.225	0.501	0.378	14.7	12.0	18.8
car7-09	0.078	0.183	0.138	11.5	13.7	15.9
car7-11	0.379	0.554	0.270	9.8	11.4	11.1
car7-12	0.538	0.269	0.145	8.7	10.0	11.7
car8-01	2.413	1.935	1.669	5.4	4.6	4.9
car8-02	0.744	0.440	0.497	10.6	8.6	7.2
car8-03	0.541	0.583	0.565	12.9	10.5	9.7
car8-04	0.921	0.889	0.454	10.9	10.0	12.1
car8-05	0.622	0.287	0.159	9.8	10.5	13.2
car8-07	0.429	0.224	0.234	11.0	12.9	11.5
car8-08	0.483	0.147	0.309	8.7	8.2	8.4
car8-10	0.887	0.155	0.120	6.1	8.4	9.2
car8-12	1.213	0.110	0.097	5.4	6.4	6.2
Nov. 1998 to Oct. 1999 averages	**0.703**	**0.469**	**0.383**	**9.4**	**9.4**	**10.1**

Deployment Code/Description	C37:2 Alkenone, μg/g			C37:3 Alkenone, μg/g		
	Trap A (275 m)	Trap B (455 m)	Trap C (930 m)	Trap A (275 m)	Trap B (455 m)	Trap C (930 m)
			Nov. 1996 to Oct. 1997			
car3-01	32.2	18.2	23.5	3.06	1.75	1.81
car3-03	12.8	10.7	11.5	0.64	0.74	0.56
car3-05	50.4	46.7	44.2	3.16	4.16	3.45
car3-07	17.5	11.9	–	2.11	1.83	–
car3-08	–	–	16.9	–	–	2.61
car3-09	11.9	11.9	–	2.20	2.46	–
car3-10	–	–	12.8	–	–	2.66

Table 2. (continued)

Deployment Code/Description	C37:2 Alkenone, μg/g			C37:3 Alkenone, μg/g		
	Trap A (275 m)	Trap B (455 m)	Trap C (930 m)	Trap A (275 m)	Trap B (455 m)	Trap C (930 m)
car4-01	8.6	13.1	15.7	0.49	1.13	1.61
car4-03	26.1	13.7	24.9	2.09	1.29	1.94
car4-05	9.4	20.5	20.6	1.19	2.88	2.86
car4-07	9.9	31.4	76.6	2.81	9.21	21.23
car4-09	13.1	60.5	–	3.74	18.07	–
car4-11	26.3	6.4	–	2.79	0.88	–
car4-13	1.2	–	–	0.07	–	–
Nov. 1996 to Oct. 1997 averages	**18.3**	**22.3**	**27.4**	**2.0**	**4.0**	**4.3**
			Nov. 1997 to Oct. 1998			
car5-01	8.0	10.7	11.1	0.51	0.61	0.58
car5-03	21.0	30.7	27.2	3.76	6.52	5.25
car5-05	12.3	22.5	39.1	1.56	2.48	4.99
car5-07	21.0	64.5	80.5	3.90	16.40	17.95
car5-09	6.4	–	77.6	0.81	–	13.94
car5-11	9.2	53.4	–	1.45	11.44	–
car5-13	7.4	–	–	0.95	–	–
car6-01	30.6	29.0	32.9	2.15	2.58	3.54
car6-03	27.4	19.1	25.3	3.31	2.19	2.88
car6-05	28.4	27.2	37.9	3.83	3.92	5.73
car6-06	23.8	29.4	–	1.39	2.54	–
car6-07	13.1	15.7	30.7	0.86	1.45	2.12
car6-09	16.2	13.3	29.2	0.76	0.45	1.24
car6-11	38.1	26.3	29.7	3.59	1.25	1.49
car6-13	10.1	–	–	0.64	–	–
Nov. 1997 to Oct. 1998 averages	**18.2**	**28.5**	**38.3**	**2.0**	**4.3**	**5.4**
			Nov. 1998 to Oct. 1999			
car7-01	5.1	15.7	22.1	0.26	0.62	0.88
car7-02	35.4	40.2	–	2.51	3.18	–
car7-03	16.2	31.6	41.6	0.62	1.24	1.77
car7-05	–	–	68.7	–	–	4.90
car7-07	–	36.3	20.5	–	4.34	2.48
car7-09	–	–	126.2	–	–	14.2
car7-11	27.1	52.1	91.9	5.61	8.23	13.4
car7-12	21.9	21.1	–	2.60	2.03	–
car8-01	–	–	6.9	–	–	0.47
car8-02	41.0	24.7	–	3.07	1.66	–
car8-03	–	–	40.9	–	–	5.17
car8-04	59.8	69.2	–	8.23	9.21	–
car8-05	–	–	44.0	–	–	6.36
car8-07	–	44.0	40.3	–	5.92	5.37
car8-08	25.7	17.4	–	2.92	1.79	–
car8-10	17.0	–	–	1.35	–	–
car8-12	11.3	–	–	0.80	–	–
Nov. 1998 to Oct. 1999 averages	**26.0**	**35.2**	**50.3**	**2.8**	**3.8**	**5.5**

[a]SST, sea surface temperature estimates derived from AVHRR satellite data collected over the study area; Avg. SST, average temperature obtained from all the valid SST satellite observations for each trap period; S.D., standard deviation of that average; n, number of satellite observations made during each time period (for some samples, n > duration days because more than one observation was made during each day; n < duration days during those periods in which cloud coverage hindered accurate satellite readings); n.d., not determined; n.r., sediment trap samples not recovered because of clogging of the sediment trap. %OC, organic carbon content; C37:2 Alkenone, diunsaturated 37:2 methylalkenone concentration; C37:3 Alkenone, triunsaturated methylalkenone concentration. All other captions are as in Table 1 and as explained in the text. Only data for those sediment traps in which alkenone measurements were made are included. A full description of the biogenic (i.e., organic carbon, carbonate, opal) compositions and fluxes of the complete set of sediment trap samples is provided by *Goni et al.* [2003].

[26] If one assumes steady state deposition [*Black*, 1998] and alkenone input, the distribution of ΣAlk_{37} in the sediments from MC-4 may be interpreted as the preferential degradation of alkenones over OC in recently deposited sediments. Alternatively, as will be discuss later, the trends observed in the surface sedimentary horizons may represent historical changes in the delivery of alkenones to the sediments from the overlying water column. Nevertheless, in order to estimate the degradation rate constant for ΣAlk_{37} in this surface sediments, we fitted the SFDW concentrations,

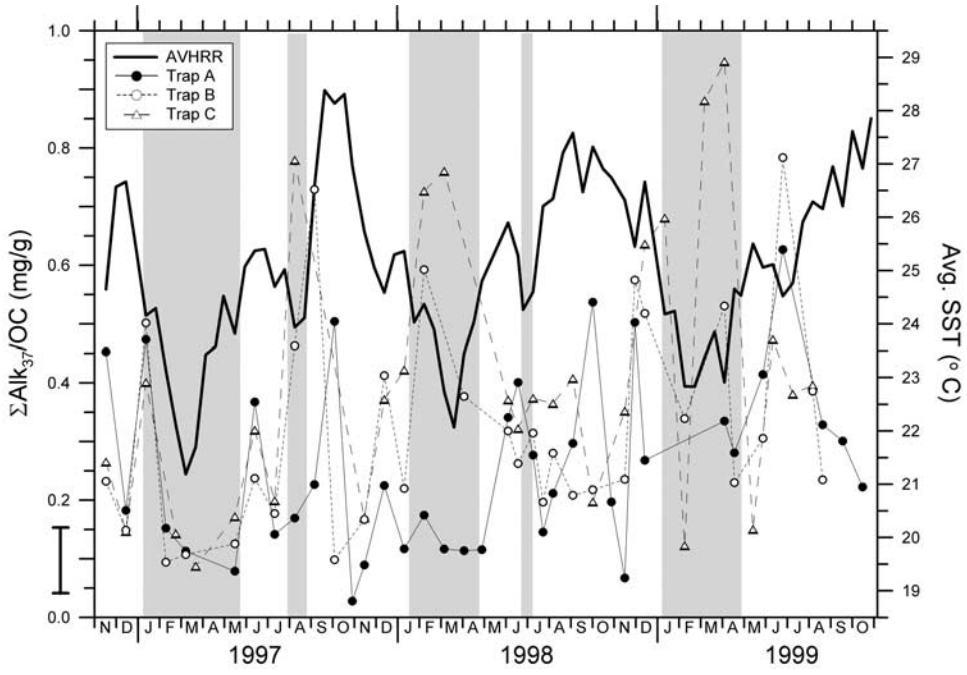

Figure 5. Ratios of total C_{37} alkenones over organic carbon concentrations (ΣAlk_{37}/OC; mg/g) in sinking particles collected in the sediment traps from different depths at the Cariaco Basin. Data are shown for Trap A (275 m), Trap B (455 m), and Trap C (930 m). Also plotted are the average sea surface temperatures (Avg. SST) determined from the AVHRR data for each of the trapping periods. All the data are from Table 2. The shaded boxes indicate upwelling periods (T < 24.5°C). The error bar adjacent to the left axis represents the average error (2 standard deviations) in the ΣAlk_{37}/OC ratio values as estimated using propagation of error based on the standard deviations of the alkenone and OC analyses.

which account for variations in porosity, to the ages of the sediments using a first-order exponential decay equation [*Sun and Wakeham*, 1994; *Westrich and Berner*, 1984],

$$G_z = G_o e^{(kt)}, \quad (4)$$

where G_z is the ΣAlk_{37} concentration at any time (t in years) after initial deposition, G_o, is the concentration at t = 0, and k is the degradation rate constant (yr^{-1}) (Figure 7b).

[27] A simple first-order 1-G model (i.e., assume one pool of alkenones with similar reactivity) successfully captured ($r^2 = 0.9$) the distribution of ΣAlk_{37} concentrations over the last 80 years of deposition (Figure 7b). The degradation rate constant for ΣAlk_{37} in the surface sediments estimated using this approach is k = -0.018 yr^{-1} (or -0.000048 d^{-1}). Individually, the degradation rates of the $C_{37:2}$ and $C_{37:3}$ alkenones estimated using this approach were -0.019 yr^{-1} and -0.011 yr^{-1}, respectively. We also used a 2-G model (i.e., two pools of alkenones with different reactivity) to calculate the decay constant for the reactive pool of alkenones in the sediments, assuming that a background of ΣAlk_{37} (1.8 μg g^{-1} SFDW) was unreactive [*Sun and Wakeham*, 1994; *Westrich and Berner*, 1984]. This approach (plot not shown) yielded a poorer fit to the data ($r^2 = 0.8$) and a higher k of -0.056 yr^{-1} (or -0.00015 d^{-1}). Similar calculations for the reactive pools of $C_{37:2}$ and $C_{37:3}$ yielded reaction rate constants of -0.063 yr^{-1} and -0.034 yr^{-1}, respectively. The data from these diagenetic models, which assume a steady alkenone accumulation history, show that in situ sediment ΣAlk_{37} degradation rate constants were 3 orders of magnitude lower than the decay rate constant estimated for these compounds during water column transport (Figure 6). Overall, our results suggest that degradation of alkenones in the anoxic sediments of the Cariaco Basin is minor relative to the losses that occur in the water column.

3.4. Alkenone Compositions in Sediments From the Gravity Core

[28] The compositions of sediments from the gravity core, CAR7-2, are presented in Table 4. The AMS ^{14}C ages indicated that the bottom of the core is ~5500 year old. The %OC content of the sediments ranged from ~5 to ~4% DW without a clear trend with depth. The concentrations of the $C_{37:2}$ and $C_{37:3}$ alkenones ranged between 6.5 to 1.7 μg/g DW and between 0.6 to 0.1 μg/g DW, respectively. The plots of SFDW concentrations versus the age of the sediments revealed a systematic decrease in the SFDW %OC content of the sediments that can be fitted to a simple first-order decay equation (equation (3)) (Figure 8). Although there was some down core variability in %OC data, the reasonable fit to the first-order decay equation ($r^2 = 0.7$) is consistent with a relatively steady accumulation and a long-term decay rate constant of -0.00005 yr^{-1}. In contrast, the ΣAlk_{37} concentration profile showed several maxima and minima suggestive of historical changes in the supply of

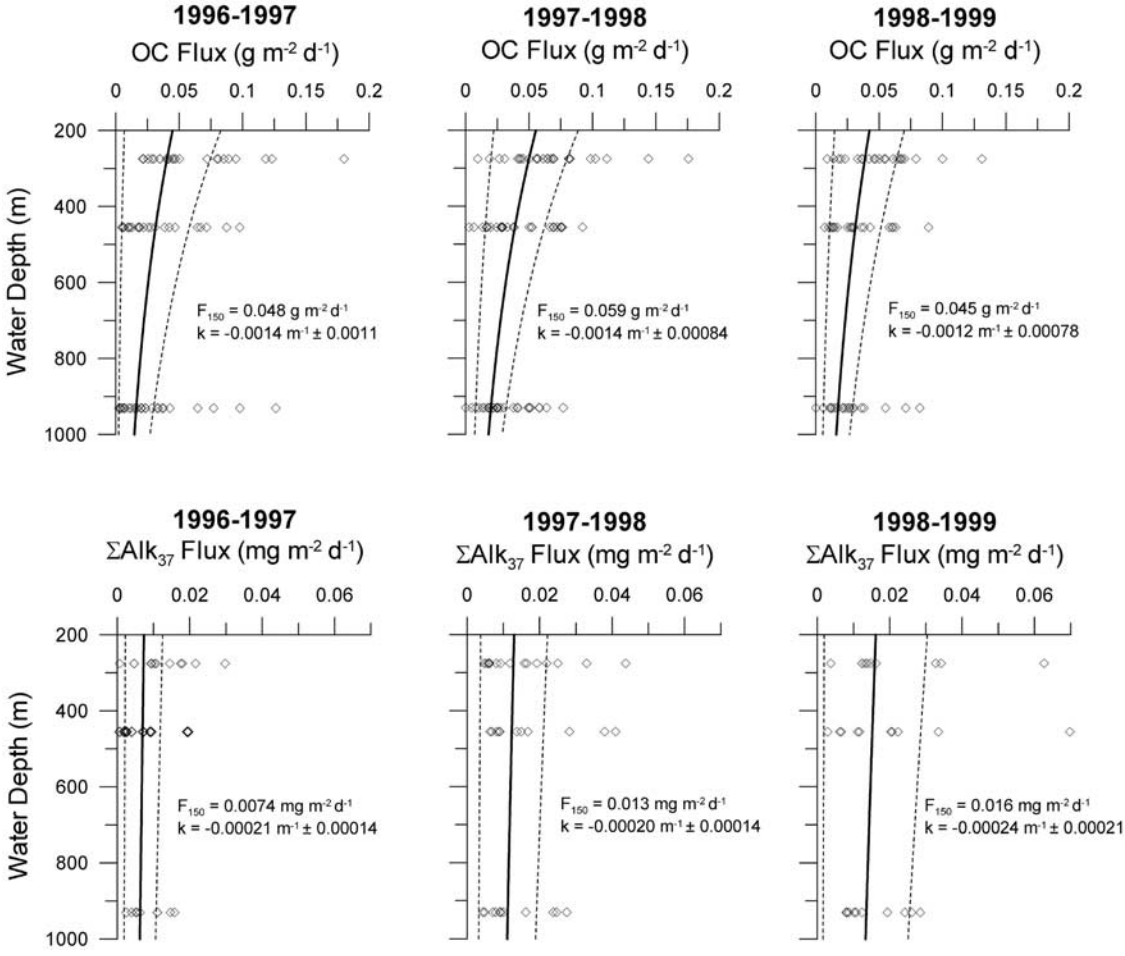

Figure 6. Fluxes of organic carbon (OC) and total alkenones (ΣAlk_{37}) measured in sediment traps at three different depths for the three separate upwelling-stratification cycles. In each of the graphs, the mean fit to the flux data estimated using the approach of *Christian et al.* [1997] is indicated by a solid line. Dashed lines indicate the variability associated with ±1 standard deviation from the mean. The resulting estimates for the flux at 150 m (F_{150}) and the decay rate constant (k) are listed in each graph. More details on the calculations are provided in the text.

alkenones to the sediments at this site. The decrease in ΣAlk_{37} measured over the last 1000 years of sediment deposition can be fitted to a first-order decay expression (equation (3)), albeit the resulting r^2 is 0.6. This calculation yielded a degradation rate constant for alkenones of $-0.00165\ yr^{-1}$. The ΣAlk_{37}/OC ratios of the gravity core sediments ranged from 0.16 to 0.04 and showed three distinct peaks at 300, 1800, and 3500–4500 ybp.

4. Discussion

[29] The results of our study reveal a large variability in the seasonal and interannual export of alkenones from the euphotic zone and in their transport and accumulation in the water column and sediments of the Cariaco Basin. Most of the trends in alkenone generation appear to be related to the changes in surface ocean temperature associated with the annual upwelling-stratification cycles in the area. We also observed significant variability in the accumulation and burial of alkenones in Cariaco basin sediments, which may be recording past changes in upwelling strength and duration as well as other factors affecting SST (e.g., ENSO frequency, global warming). However, some of these trends may be due to post-depositional diagenetic alteration rather than climatic and oceanographic variability. In this respect, we observed large differences in the calculated decay rate constants of alkenones between the water column and sediments. For example, the degradation rate constant obtained from the top horizons of the gravity core sediments ($k = -0.0017\ yr^{-1}$), which represent ~1000 years of sedimentation, is an order of magnitude lower than the k ($-0.018\ yr^{-1}$) obtained from the surface 8 cm of the multicore sediments, which represent ~100 years of accumulation. In contrast, the decay of alkenones during their transport through the water column are consistent with much more rapid degradation ($k \approx -7.3\ yr^{-1}$). The observation that the magnitude of the decay constant estimated depends on the timescale of the measurement is consistent with previous studies (see review by *Henrichs* [1997]) and indicates that the lability of alkenones is most likely a

Table 3. Compositions of Multicore Sediments MC-4[a]

Depth, cm		Age,	Porosity,	%OC,	$C_{37:2}$,	$C_{37:3}$,
Top	Bottom	ybp	cm^3/cm^3	wt.% DW	μg/g DW	μg/g DW
0.0	0.5	5	0.93	5.19	5.15	0.479
0.5	1.0	10	0.93	4.47	2.87	0.199
1.0	1.5	14	0.93	4.40	3.58	0.247
1.5	2.0	19	0.93	5.17	3.37	0.253
2.0	2.5	23	0.92	5.50	3.27	0.250
2.5	3.0	28	0.92	5.07	3.39	0.238
3.0	3.5	32	0.92	4.82	1.93	0.145
3.5	4.0	38	0.92	4.93	2.99	0.226
4.0	4.5	42	0.92	5.26	3.27	0.301
4.5	5.0	44	0.92	5.02	2.58	0.234
5.0	5.5	46	0.91	5.32	2.72	0.259
5.5	6.0	49	0.91	5.50	2.12	0.201
6.0	6.5	52	0.91	5.32	2.20	0.214
6.5	7.0	57	0.91	5.53	1.66	0.174
7.0	7.5	61	0.91	5.24	1.64	0.211
7.5	8.0	66	0.91	5.06	1.46	0.181
8.0	8.5	72	0.90	5.33	1.44	0.174
8.5	9.0	74	0.90	5.33	1.93	0.248
9.0	10	77	0.90	5.72	2.48	0.286
9.5	10	80	0.90	5.28	2.43	0.312
10	11	84	0.90	5.64	1.82	0.243
11	12	96	0.89	5.49	2.06	0.252
12	13	107	0.89	5.32	1.48	0.159
13	14	116	0.89	5.30	1.79	0.199
14	15	125	0.89	5.08	2.28	0.182
15	16	135	0.89	4.76	2.38	0.329
16	17	144	0.88	4.85	2.16	0.256
17	18	154	0.88	5.65	2.36	0.278
18	19	164	0.88	5.27	2.71	0.312
19	20	175	0.88	5.61	2.16	0.244
20	21	185	0.88	5.75	2.55	0.290
21	22	196	0.88	5.51	3.40	0.413
22	23	207	0.87	4.95	n.m.	n.m.
23	24	219	0.87	5.21	2.07	0.253
24	25	230	0.87	5.63	2.41	0.311
25	26	242	0.87	6.10	2.13	0.255
26	27	255	0.87	4.70	1.76	0.215
27	28	267	0.87	5.53	1.77	0.221
28	29	280	0.87	5.80	1.57	0.207
29	30	293	0.87	5.38	1.33	0.145
30	31	307	0.87	5.22	1.05	0.105

[a]Ages based on sedimentation rates determined by *Black* [1998] for this area of the Cariaco Basin; ybp, years before present. Porosity calculated from water content measurements, bottom water salinity (36.32 ppt), and particle density (2.1 g cm^{-3}); %OC, weight percent organic carbon; $C_{37:2}$, diunsaturated C_{37} methyl ketone concentration; $C_{37:3}$, triunsaturated C_{37} methyl ketone concentration.

continuum that depends on their diagenetic history. The trends in the sediments may also reflect nonsteady state deposition of alkenones indicative of historical variability in the productivity of haptophyte algae related to past oceanographic changes. In the next sections, we explore how the timing of alkenone generation and extent of alkenone degradation control the composition and alteration of the $\mathbf{U}^{\mathbf{K}'}_{37}$ parameter and its utility as a recorder of SST in the Cariaco Basin.

4.1. Generation and Export of the $\mathbf{U}^{\mathbf{K}'}_{37}$ Index

[30] The alkenone-based $\mathbf{U}^{\mathbf{K}'}_{37}$ ratios of sinking particles in the Cariaco Basin exhibit significant seasonal changes, ranging from 0.78 to 0.96 (Figure 9). Overall, the variability of the $\mathbf{U}^{\mathbf{K}'}_{37}$ signatures from samples collected at different depths during the same period is less than ±0.01, which is within the analytical error. In certain cases, the difference in the $\mathbf{U}^{\mathbf{K}'}_{37}$ signal is as high as 0.05 units (i.e., May 1997). For the most part, the seasonal trends in $\mathbf{U}^{\mathbf{K}'}_{37}$ are coherent with the observed changes in SST (Figure 9). During upwelling periods when SST fall below 25°C, the $\mathbf{U}^{\mathbf{K}'}_{37}$ values range between 0.8 and 0.9. In contrast, during periods of high thermal stratification when SST values reach above 26°C, $\mathbf{U}^{\mathbf{K}'}_{37}$ values peak above 0.95 (Figure 9). Thus our results indicate that for the most part, the alkenone signature of sinking particles in the Cariaco Basin appears to be generated by phytoplankton inhabiting the surface layer of the water column. Such observation is consistent with the measured productivity and pigment profiles (Figure 3), which clearly show that during the majority of the year the maxima in primary production and chlorophyll are located in the upper 25 m of the water column [*Goni et al.*, 2003]. The major exceptions were during August and September of 1997, December of 1997, and February of 1998, when the $\mathbf{U}^{\mathbf{K}'}_{37}$ values corresponded to temperatures significantly lower than the SST. These periods coincided with the passage of anticyclonic and cyclonic eddies over the Cariaco Basin [*Astor et al.*, 2003], which clearly affected the alkenone temperature signal recorded in these traps.

[31] In order to test the effectiveness of the alkenone-based temperature index, we plotted the $\mathbf{U}^{\mathbf{K}'}_{37}$ values measured in trap samples versus the average SST estimated for each sample (Figure 10). As can be seen, most of the samples plot along the calibration line of *Prahl et al.* [1988] ($\mathbf{U}^{\mathbf{K}'}_{37}$ = 0.034T + 0.039), which was determined for *E. huxleyi* in laboratory cultures. There is considerable spread of the data, with the largest deviations observed for those samples collected during periods of eddy passage. One possible explanation for these contrasts is that lateral eddies introduce other species of alkenone-producing phytoplankton, such as *G. oceanica*, with different unsaturation response to temperature (e.g., $\mathbf{U}^{\mathbf{K}'}_{37}$ = 0.049T − 0.520 [*Volkman et al.*, 1995]. However, this explanation would necessitate that the majority of the haptophyte algae brought in by eddies be of different species composition than the populations normally present in Cariaco. We do not have coccolith species data for these trap samples, but such contrasts in species composition seems unlikely given the observations that *E. huxleyi* dominates the coccolithophore assemblage throughout the Caribbean Sea with minor contributions from *G. Oceanica* [*Winter et al.*, 2002]. A more likely explanation is that during lateral water intrusions, phytoplankton growing deeper in the water column of the Caribbean Sea are imported into the basin. Indeed, the chlorophyll maximum in the Caribbean Sea is typically located 50 to 100 m below the surface [*Corredor and Morell*, 2001]. Furthermore, coccolithophore species such as *E. huxleyi* are abundant in the subsurface. Hence, under this scenario, the alkenones reaching the traps during eddy passage are probably recording deeper temperatures outside the basin, rather than the SST they normally reflect during the rest of the time.

[32] The other major observation that can be made from Figure 10 is that the samples obtained during upwelling periods appear to display higher variability versus SST than those collected during non-upwelling periods. Most obvious

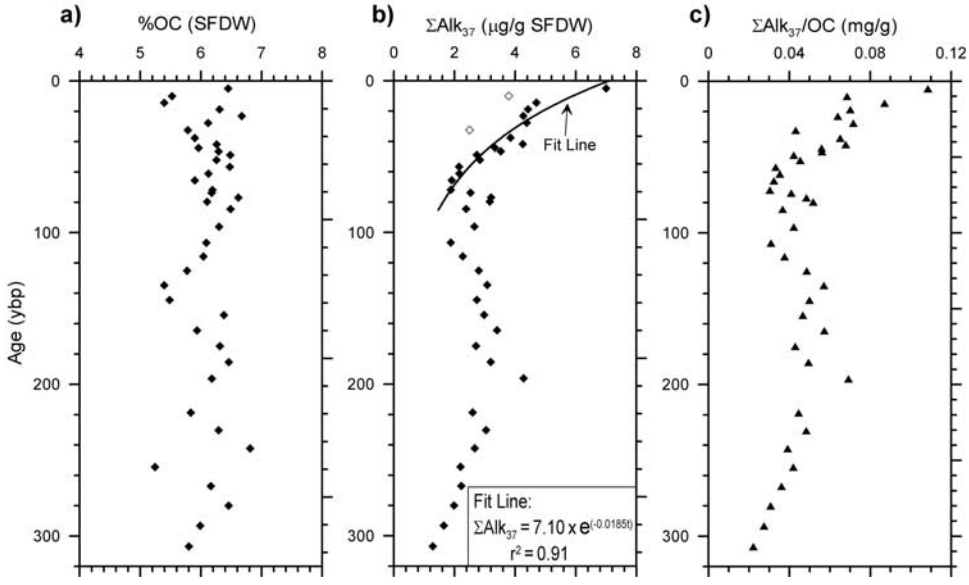

Figure 7. Compositions of sediments from MC-4 versus sediment age: (a) weight percent organic carbon content as salt-free dry weight (%OC SFDW); (b) total C_{37} alkenone concentrations concentrations in units corrected for salt content (ΣAlk_{37} μg/g SFDW); (c) ΣAlk_{37}/OC ratios (mg/g). All data are from Table 3. The correction for salt content was applied to the DW OC and ΣAlk_{37} databased on porosity and using a value for bottom water salinity of 36.32 ppt and a sediment density of 2.1 g cm^{-3}. Included in Figure 7b is a fit to the ΣAlk_{37} concentrations from the top of the core using a simple 1-G exponential decay equation. The resulting equation is included in the figure. The data points highlighted in the open symbols were not included in this calculation. More details on the calculations are provided in the text.

are the larger than expected $\mathbf{U^{K'}_{37}}$ values obtained when SST falls below ~25°C. This trend may be attributed to the time lag between the temperature of the surrounding water column and the export of the alkenone signature out of the euphotic zone. During upwelling periods when SST changes very quickly, this lag becomes most evident because alkenone-producers cannot acclimate quickly enough to the rapid temperature changes. Thus the temperature signal recorded in the sinking flux collected over a 2-week period partially reflects temperature conditions prior to those present during sample collection. Time lags have been invoked in other sediment trap studies to account for the time difference between production and collection [*Prahl et al.*, 2000a; *Steinberg et al.*, 2001]. In this case, the traps are located at relatively shallow depths and we do not observe a systematic trend among the three traps. Hence we attribute most of the lag to the acclimatization period of alkenone producers to temperature changes and their export (presumably by grazing) out of the euphotic zone, rather than to lags associated with the sinking time of particles.

[33] In order to account for the likely allocthonous provenance of alkenones during periods of eddy passage, we plotted the alkenone index versus subsurface temperatures (~50 m below the surface) for those samples collected during August, September, October, and December 1997 and February 1998 (Figure 11). Such correction reflects our interpretation that in periods during and following lateral intrusions, materials are imported into the basin with signatures that reflect conditions in the Caribbean Sea, which likely include deeper alkenone production in the water column. The other major correction we made was to apply a 7-day time lag to the samples collected during upwelling periods. Accordingly, we plotted the $\mathbf{U^{K'}_{37}}$ signatures of upwelling samples versus the average SST estimated for the 2-week period that started 7 days prior to when the cups opened. The result of these corrections is a significant tightening of the relationship between $\mathbf{U^{K'}_{37}}$ and SST (Figure 11), which closely overlaps with the expression of *Prahl et al.* [1988]. Hence we conclude that the generation of alkenones by haptophyte algae during different seasons in the Cariaco Basin is consistent with the trends observed in laboratory cultures of *E. huxleyi* and that the $U^{K'}_{37}$ ratios in sinking particles are an acceptable proxy of the seasonal trends in SST. The fact that the relationship between $\mathbf{U^{K'}_{37}}$ and SST holds in the deeper traps, which receive diminished alkenone fluxes due to water column decay (Figure 6), is consistent with the robustness of this proxy through the early stages of diagenesis.

[34] In order to quantify the effectiveness of alkenones to reconstruct the SST history in the Cariaco Basin, it is necessary to confirm that the annual $\mathbf{U^{K'}_{37}}$ signal exported to the sediments reflects the mean annual temperature of the surface ocean. With that objective in mind, we calculated the cumulative fluxes of the $C_{37:2}$ and $C_{37:3}$ compounds in each of the three traps for the three annual periods (Table 5). Using these cumulative fluxes, we estimated the flux-weighed annual $\mathbf{U^{K'}_{37}}$ ratios for each trap and then used the calibration equation of *Prahl et al.* [1988] to estimate the SST signature

Table 4. Gravity Core (CAR 7-2) Sediment Data[a]

Depth, cm		^{14}C Age,	Porosity,	%OC,	$C_{37:2}$,	$C_{37:3}$,
Top	Bottom	ybp	cm^3/cm^3	wt.% DW	μg/g DW	μg/g DW
1.0	1.5	300	0.89	4.98	6.51	0.631
5.0	5.5	457	0.88	4.97	3.77	0.285
10.0	10.5	678	0.87	5.14	3.38	0.189
15.0	15.5	761	0.86	5.32	4.00	0.338
19.0	19.5	776	0.86	4.95	3.93	0.242
25.0	25.5	835	0.85	4.92	1.67	0.095
30.0	30.5	892	0.84	4.78	2.33	0.175
36.0	36.5	981	0.83	5.30	2.66	0.184
40.0	40.5	1046	0.83	5.37	3.24	0.222
45.0	45.5	1130	0.82	5.12	2.42	0.137
50.0	50.5	1217	0.82	5.32	4.03	0.246
59.0	59.5	1378	0.81	4.85	3.42	0.290
70.0	70.5	1598	0.80	5.18	6.15	0.535
78.0	78.5	1768	0.79	4.82	7.43	0.546
89.5	90.0	2000	0.79	5.25	5.61	0.443
100.0	100.5	2205	0.79	4.97	3.77	0.324
110.0	110.5	2408	0.79	4.63	3.57	0.302
120.0	120.5	2610	0.79	5.03	2.74	0.241
130.0	130.5	2811	0.79	4.78	3.05	0.304
140.0	140.5	3049	0.79	4.53	2.19	0.155
150.0	150.5	3286	0.79	4.35	3.37	0.283
160.0	160.5	3521	0.79	4.10	4.82	0.432
170.0	170.5	3817	0.79	4.31	4.95	0.395
180.0	180.5	4112	0.79	4.07	4.26	0.269
190.0	190.5	4405	0.79	4.55	5.33	0.372
200.0	200.5	4771	0.79	4.59	3.90	0.291
210.0	210.5	5134	0.79	4.33	3.59	0.248
220.0	220.5	5494	0.79	4.31	3.20	0.277

[a] ^{14}C Age and are based on the data and age model of *Black et al.* [2001]; porosity was calculated based on the dry bulk density data [*Black et al.*, 2001] assuming a pore water salinity of 36.32 ppt and a particle density of 2.1 g cm^{-3}; %OC, weight percent organic carbon; $C_{37:2}$, diunsaturated C_{37} methyl ketone concentration; $C_{37:3}$, triunsaturated C_{37} methyl ketone concentration.

expected from the alkenone fluxes recovered in each trap over each annual period. A comparison of the $\mathbf{U^{K'}_{37}}$-based SST estimates from trap A with the average satellite-derived SST measurements for the same periods shows that the two temperatures are within 0.5°C of each other (Table 5). The differences in SST estimates are greater for traps B and C, especially during 1997–1998. The effect of the cyclonic and anticyclonic eddies on the alkenone flux and $\mathbf{U^{K'}_{37}}$ appears to be the major reason for this discrepancy. For example, by excluding the periods in December 1997 and February 1998 from the above calculations, the ΔSST differences are reduced to less than 0.6°C for all three traps for the 1997–1998 period. Overall, our results indicate that the alkenones exported from the euphotic zone provide an accurate quantitative estimate of SST (±0.5°C) and that this signal is eroded somewhat during transport through the water column, so that the deeper traps display slightly greater variability (±0.8°C). This conclusion is consistent with the earlier findings of *Herbert and Schuffert* [2000] in which they concluded that the $\mathbf{U^{K'}_{37}}$ signal preserved in Cariaco Basin surface sediments is an accurate indicator of mean annual SST.

4.2. Preservation of the $\mathbf{U^{K'}_{37}}$ Index in Sediments and SST Reconstructions

[35] In order to successfully apply alkenone-paleothermometry to reconstruct the temperature history of the Cariaco Basin, we need to assume that the signal preserved in sediments has not changed after its initial deposition. Furthermore, we also need to assume that the timing and depth of alkenone production and export have not changed much in the time interval covered by the sediments. For example, if in the past alkenone-producers showed a more seasonal biased distribution or lived at greater depths in the water column than they do at present, the interpretation of the SST records may be incorrect. Testing these assumptions is difficult under the best circumstances. Nevertheless, in this section we contrast the records of ΣAlk_{37} accumulation to the trends in $\mathbf{U^{K'}_{37}}$ compositions to investigate coherent trends that are consistent with the patterns of alkenone generation in modern day Cariaco Basin. *Goni et al.* [2003] showed that between 1996 and 1999 the annual flux of alkenones out of the euphotic zone correlated positively with annual mean SST, whereas annual opal flux showed the opposite trend, with the highest annual fluxes occurring during the years with lowest mean SST. These observations are consistent with the dominance of diatoms in the particle export during periods of strong upwelling and the enhanced importance of haptophyte algae during periods of low upwelling. Therefore our expectation is that during past intervals of diminished upwelling, we should observe enhanced ΣAlk_{37} fluxes and elevated $\mathbf{U^{K'}_{37}}$ consistent with higher mean annual SSTs.

[36] The ΣAlk_{37} accumulation flux data and $\mathbf{U^{K'}_{37}}$ compositions obtained from the combined records in MC-4 and CAR-7 are generally consistent with our expectations and indicate that alkenones provide a reliable record of mean SST conditions in the Cariaco Basin over the past 6000 years (Figure 12). There are several interesting features of these data that are worth discussing in more detail. For example, the $\mathbf{U^{K'}_{37}}$ compositions in sediments deposited over the past 50 years indicate the mean SST for this period was significantly higher (26.3°C) than the mean SST (~25.1°C) during 1993–2001 (Figure 12b). Furthermore, the ΣAlk_{37} burial fluxes during this period are relatively high (Figure 12a), lending support to the scenario that diminished upwelling during this period may have favored haptophyte productivity in the surface waters of the basin. Most notably, our data and interpretation are consistent with a recent coralline trace element study of *Reuer et al.* [2003], which demonstrated a significant reduction in upwelling in the Cariaco Basin since the beginning of the middle of the twentieth century. One of the consequences of this interpretation is that the changes in alkenone concentrations in the top portion of MC-4 (Figure 7b) are likely to be partially attributed to variations in the delivery of these compounds. Hence the degradation rate constant estimated from the concentration profile is likely to be an overestimation since alkenone fluxes probably increased over the last 100 years.

[37] The lowest temperatures (~25°C) estimated from the combined sedimentary record occur between 100 and 400 ybp (Figure 12b). This time interval, which is often referred as the little ice age (LIA), is also characterized by relatively low ΣAlk_{37} burial fluxes (Figure 12a). Thus we conclude that during this period upwelling was enhanced leading to a decrease in the production and export of alkenone-producing haptophyte algae and overall lower

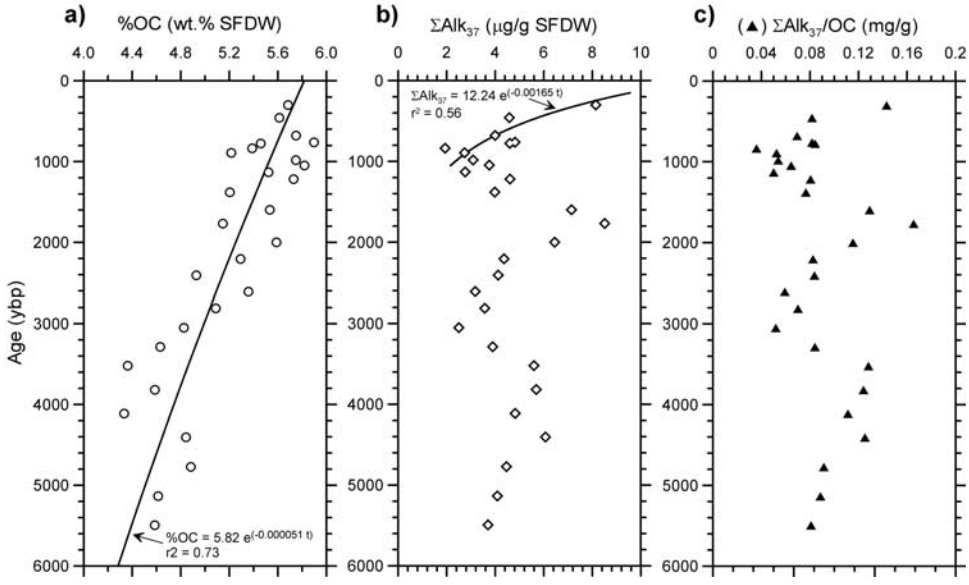

Figure 8. Compositions of sediments from CAR7-2 versus sediment age: (a) weight percent organic carbon content as salt-free dry weight (%OC SFDW); (b) total C_{37} alkenone concentrations in units corrected for salt content (ΣAlk_{37} μg/g SFDW); (c) ΣAlk_{37}/OC ratios (mg/g). All data are from Table 4. The correction for salt content was applied to the DW OC and ΣAlk_{37} databased on porosity and using a value for bottom water salinity of 36.32 ppt and a sediment density of 2.1 g cm^{-3}. Figure 8a includes an exponential fit to the %OC a simple 1-G exponential decay equation. A similar fit is included in Figure 8b for the ΣAlk_{37} concentrations from the top of the core. The resulting equations are included in the figure. More details on the calculations are provided in the text.

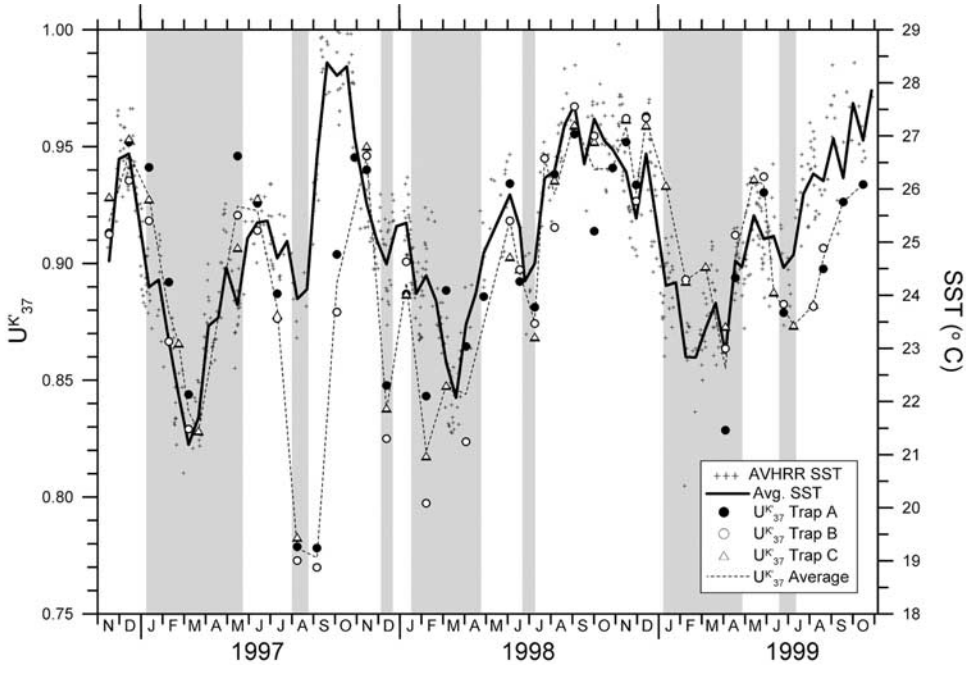

Figure 9. Alkenone-based $U_{37}^{K'}$ ratios in sinking particles collected in the sediment traps from different depths at the Cariaco Basin. Data are shown for all three traps. Also plotted are the individual sea surface temperatures SST measurements determined from the AVHRR (AVHRR SST) and average SST (Avg. SST) data for each of the trapping periods. All the data are from Table 2. The shaded boxes indicate upwelling periods (T < 24.5°C).

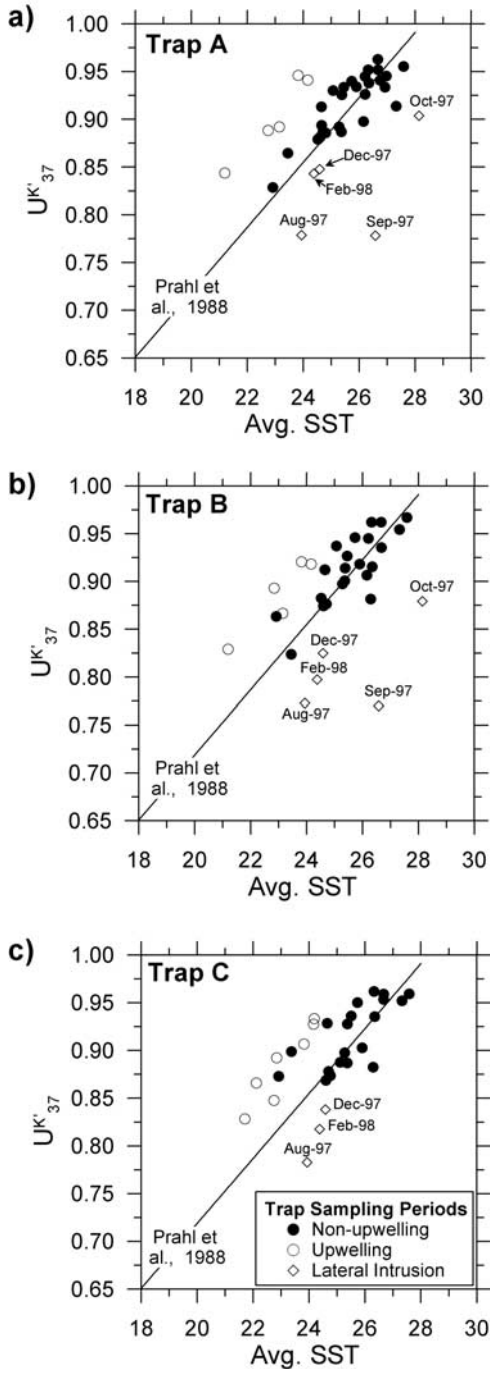

Figure 10. Plots of the alkenone-based $U^{K'}_{37}$ ratios of sinking particles collected by sediment traps versus the average SST for each collection period. Data are presented for traps (a) A, (b) B, and (c) C. In each plot, the calibration equation determined by *Prahl et al.* [1988] from culture studies is included for reference. Samples collected during different periods (non-upwelling, upwelling, and lateral intrusions) are plotted with different symbols.

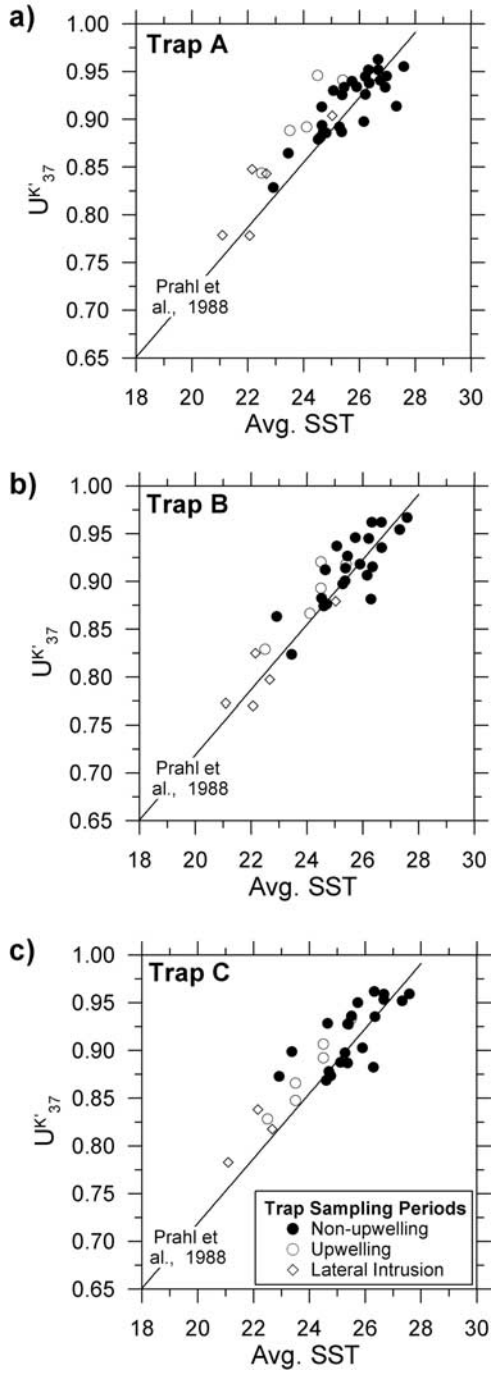

Figure 11. Plots of the alkenone-based $U^{K'}_{37}$ ratios of sinking particles versus average SST after corrections for the effects of lateral intrusions due to eddies and time lags associated with phytoplankton acclimatization and alkenone export. Details of the corrections are discussed in the text. Data are presented for traps (a) A, (b) B, and (c) C In each plot, the calibration equation determined by *Prahl et al.* [1988] from culture studies is included for reference. Samples collected during different periods (non-upwelling, upwelling, and lateral intrusions) are plotted with different symbols.

surface ocean temperatures. The rest of the sedimentary record yielded SST estimates that exceed those measured during the LIA. The highest temperature estimates (>26.5°C) occur between ~600 and 1200 ybp, which

Table 5. Cumulative Alkenone Water Column Fluxes and Compositions[a]

Trap	# Trap Days	$C_{37:2}$ Flux, μg m^{-2} d^{-1}	$C_{37:3}$ Flux, μg m^{-2} d^{-1}	$U^{K'}_{37}$	$U^{K'}_{37}$-SST, °C	SST, °C	ΔSST, °C
			1996–1997				
Trap A	147	12.3	1.51	0.89	25.1	24.8	0.3
Trap B	147	6.3	1.10	0.85	23.9	24.8	−0.8
Trap C	147	5.8	0.86	0.87	24.5	24.0	0.5
			1997–1998				
Trap A	159	15.1	1.62	0.90	25.4	25.7	−0.2
Trap B	147	15.1	2.48	0.86	24.1	25.6	−1.4
Trap C	133	11.9	1.75	0.87	24.5	25.4	−0.9
			1998–1999				
Trap A	154	17.8	1.81	0.91	25.6	25.5	0.1
Trap B	154	16.8	1.85	0.90	25.3	25.1	0.2
Trap C	140	14.2	1.44	0.91	25.6	24.8	0.8

[a] $C_{37:2}$ and $C_{37:3}$ fluxes represent the daily average fluxes calculated by dividing the cumulative fluxes collected in each trap by the number of trapping days. In some cases the number of trap days differs between traps of the same year because a different number of samples was analyzed (see Table 2). The cumulative $U^{K'}_{37}$ index for each year and each trap was calculated using the daily cumulative fluxes in the table. $U^{K'}_{37}$-SST, alkenone-based sea surface temperature calculated using the expression of *Prahl et al.* [1988] ($U^{K'}_{37}$ = 0.034T + 0.039); SST, represents the satellite-derived average sea surface temperature calculated for the period each of the traps was open; ΔSST, difference between alkenone-based and satellite-based SST estimates.

coincides with the Medieval Warm Period (MWP). These temperatures are also comparable to those estimated for the last 50 years at this site and probably indicate reduced upwelling. Similarly high $\mathbf{U^{K'}_{37}}$ temperatures were estimated for the last interglacial (isotope stage 5e) in Cariaco Basin ODP site 1002 [*Herbert and Schuffert*, 2000]. Furthermore, the elevated ΣAlk_{37} burial fluxes measured from 800 to ~2500 ybp (Figure 12a) are consistent with this interpretation. Prior to ~1400 ybp, the alkenone record is fairly stable, with temperatures varying within ~0.5°C of 26°C and ΣAlk_{37} burial fluxes averaging 2 mg m^{-2} d^{-1}. These compositions suggest that this period was characterized by stronger upwelling conditions relative to those during the last 50 years and the MWP but by SSTs that were higher than during the LIA. This overall pattern of temperature change during the middle to late Holocene in Cariaco Basin is similar to that previously reported by *Herbert and Schuffert* [2000] for ODP Site 1002 (10.71°N; 65.17°W). Their low-resolution $\mathbf{U^{K'}_{37}}$-SST record shows uniform temperature of 25.5° to 26.0°C from 6000 to 2000 ybp, followed by a 1°C cooling during the last 2000 years.

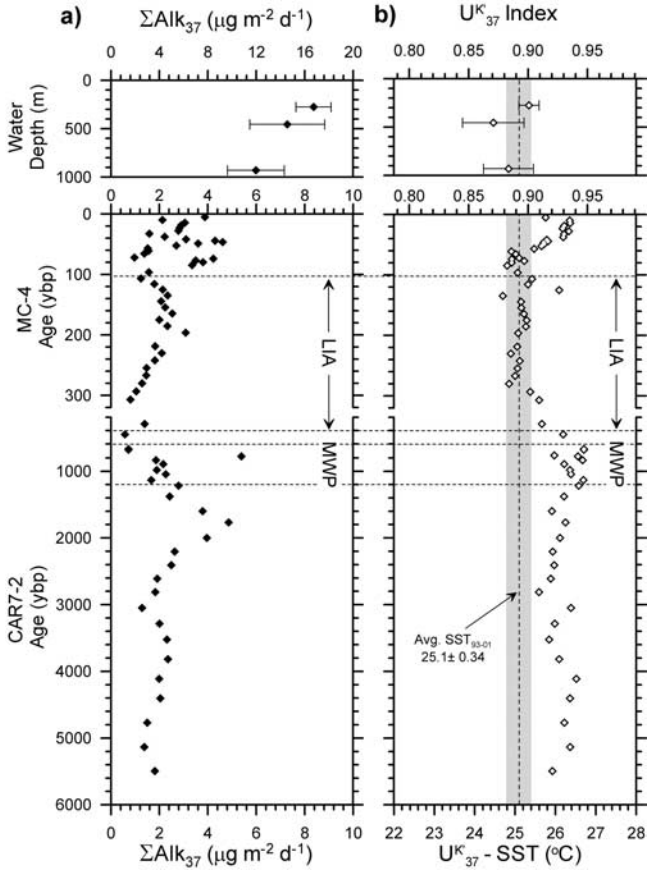

Figure 12. (a) Accumulation fluxes of total C_{37} alkenones and (b) alkenone-based $\mathbf{U^{K'}_{37}}$ ratios in the water column and sediments of the Cariaco Basin. Note the difference in units between the ΣAlk_{37} flux axis for the sediment trap and sediment data. In the $\mathbf{U^{K'}_{37}}$ graph, the corresponding SST calculated using the *Prahl et al.* [1988] equation is plotted in the bottom axis. The data plotted include the flux-weighed averages from the 3 years of sediment trap collections (Table 2), from the MC-4 sediments (Table 3), and the CAR7-2 sediments (Table 4). The error bars in the sediment trap data represents the interannual variability in these parameters. The average and standard deviation in SST determined from the 1993–2001 AVHRR SST record (Figure 2) is included for reference in the $\mathbf{U^{K'}_{37}}$ graph.

4.3. Comparison With Other Records of Climate Change From Cariaco Basin

[38] If one assumes that the annual temperature signal of the surface ocean in the Cariaco Basin has been mainly controlled by trade wind intensity, as it does under present-day conditions, we can compare our alkenone results with the recent findings of *Haug et al.* [2001]. Using Ti concentrations in Cariaco Basin sediments, these authors concluded that the ITCZ has migrated to the south during the last 6000 years. This shift in the ITCZ has resulted in

decreased precipitation, stronger trade winds and increased occurrence of El Niño during the latter half of the Holocene. Our alkenone observations indicate that trade wind intensity increased in the Cariaco Basin during the LIA (~100–400 ybp) relative to conditions during the preceding MWP. Similarly, Ti concentrations are higher during the MWP than the LIA, indicating that the LIA was drier and had stronger trade winds that the MWP [*Haug et al.*, 2001]. Our results also suggest that trade wind intensity was reduced during the MWP and during the most recent 50 years, leading to less intense upwelling and higher mean SSTs in the basin that reached 27°C. Between 2000 and 5600 ybp, trade wind intensities must have been higher than during the MWP, with slight variations that maintained mean SSTs of ~26°C.

[39] There remains an unanswered question regarding the application of the $\mathbf{U}^{\mathbf{K}'}_{37}$ paleothermometer to the Pleistocene temperature history of Cariaco Basin. In their study of ODP Site 1002, *Herbert and Schuffert* [2000] reported little temperature change associated with the last two periods of deglaciation (Terminations 1 and 2). In contrast, a recent study of planktonic foraminiferal Mg/Ca changes across termination 1 indicates a 3°C glacial-interglacial change in SST in Cariaco Basin [*Lea et al.*, 2003]. In order to resolve this discrepancy, a multiproxy study ($\mathbf{U}^{\mathbf{K}'}_{37}$, Mg/Ca, and $\delta^{18}O$) carried out on a Cariaco Basin sediment core is needed to evaluate the internal consistency of these different paleothermometers. Comparisons between glacial/interglacial periods need to take into account the significant hydrographic changes that occurred inside the Cariaco Basin due to the decreased sea level during glacials, which led to enhanced isolation from the open Caribbean, lower productivity and oxic bottom waters [*Herbert and Schuffert*, 2000; *Yarincik et al.*, 2000]. In this respect, it is important to note that the findings from our study apply to a high sea level conditions during which regional upwelling induced by the seasonal migration of the ITCZ is readily expressed inside the Cariaco Basin. Under these conditions, upwelling-induced SST changes are accurately captured in the well-preserved alkenone record of anoxic sediment, a scenario that may not necessarily apply to periods of low sea level.

5. Summary

[40] The fluxes and compositions of alkenones in sinking particles from the Cariaco Basin show that the generation and transfer of the $\mathbf{U}^{\mathbf{K}'}_{37}$ index from the euphotic zone to the underlying sediments over several seasonal upwelling-stratification cycles agrees well with previously published laboratory and field calibration studies [*Müller and Fischer*, 2001; *Müller et al.*, 1998; *Prahl et al.*, 1988]. The alkenone-based temperature proxy is responsive to rapid temperature changes and, after accounting for the effects of time lags and lateral water intrusions, successfully reproduces the annual SST signal in the Cariaco Basin. The transfer of the $\mathbf{U}^{\mathbf{K}'}_{37}$ index through the water column and sediments occurs with minor erosion of its paleotemperature reconstruction potential, yielding estimates of SST and upwelling strength that are consistent with previously published results. Thus the alkenone burial flux and $\mathbf{U}^{\mathbf{K}'}_{37}$ index records from Cariaco Basin sediments reveal important historical changes in the strength of upwelling and annual SST conditions over late to middle Holocene. Significantly reduced upwelling conditions characterize the most recent 50 years of accumulation history at the site, as well as the medieval warm period, relative to the conditions present during the little ice age. The alkenone signatures of sediments from the latter period indicate conditions of enhanced upwelling, significantly lower SSTs and reduced haptophyte production. Finally, the alkenone reconstructions suggest that the conditions at the Cariaco basin from ~2000 to ~6000 ybp were characterized by slightly reduced upwelling relative to the LIA and lower SSTs than the MWP. These findings corroborate the utility of alkenones and the $\mathbf{U}^{\mathbf{K}'}_{37}$ index to reconstruct past oceanographic conditions, even in areas where changes in SST are as dynamic as in this upwelling dominated region of the Caribbean Sea and where alkenone degradation in the water column and sediments destroy over 90% of the export flux.

[41] **Acknowledgments.** We thank the personnel from the Estacion de Investigaciones Marinas de la Fundacion La Salle for logistical support and the captain and crew of the *Buque Oceanografico Hermano Gines* for their invaluable assistance at sea. This research was funded through National Foundation grants to R. Thunell and M. Goni (OCE 9729697 and OCE 0118349) and to F. Müller-Karger (OCE 9729284) and through the support of the Consejo Nacional de Investigaciones Cientificas y Tecnologicas (CONICIT, Venezuela, grant 96280221). This paper benefited from the reviews and comments of three anonymous reviewers.

References

Astor, Y., F. Müller-Karger, and M. I. Scranton (2003), Seasonal and interannual variation in the hydrography of the Cariaco Basin: Implications for basin ventilation, *Cont. Shelf Res.*, *23*, 125–144.

Bard, E. (2001), Comparison of alkenones estimates with other paleotemperature proxies, *Geochem. Geophys. Geosyst.*, *2*, Paper number 2000GC000050. (Available at http://gcubed.magnet.fsu.edu/main.html)

Berner, R. A. (1980), *Early Diagenesis*, 241 pp., Princeton Univ. Press, Princeton, N. J.

Bijma, J., M. Altabet, M. Conte, H. Kinkel, G. J. M. Versteegh, J. K. Volkman, S. G. Wakeham, and P. P. Weaver (2001), Ecological and environmental factors: Report from Working Group 2, *Geochem. Geophys. Geosyst.*, *2*, Paper number 2000GC000051. (Available at http://gcubed.magnet.fsu.edu/main.html)

Black, D. E. (1998), Decadal- to century-scale climate variability in the tropical North Atlantic as recorded in sediments from the anoxic Cariaco Basin, Venesuela, Ph.D. dissertation thesis, 380 pp., Univ. of Miami, Coral Gables, Fla.

Black, D. E., L. C. Peterson, J. T. Overpeck, A. Kaplan, M. N. Evans, and M. Kashgarian (1999), Eight centuries of North Atlantic Ocean atmosphere variability, *Science*, *286*, 1709–1713.

Black, D. E., R. C. Thunell, A. Kaplan, K. A. Tedesco, E. J. Tappa, and L. C. Peterson (2001), Late Holocene tropical Atlantic climate variability: Records from the Cariaco Basin, *Eos Trans. AGU*, *82*(47), Fall Meet. Suppl., Abstract PP22B-01.

Christian, J. R., M. R. Lewis, and D. M. Karl (1997), Vertical fluxes of carbon, nitrogen, and phosphorous in the North Pacific Subtropical Gyre near Hawaii, *J. Geophys. Res.*, *102*, 15,667–15,677.

Conte, M. H., A. Thompson, G. Eglinton, and J. C. Green (1995), Lipid biomarker diversity in the coccolithophorids *Emiliania huxleyi* (PRYMNIESIOPHYCEAE) and the related species *Gephyrocapsa oceanica*, *J. Phycol.*, *31*, 272–282.

Conte, M. H., A. Thompson, D. Lesley, and R. P. Harris (1998), Genetic and physiological influences on the alkenone/alkenoate versus growth temperature relationship in Emiliania huxleyi and Gephyrocapsa oceanica, *Geochim. Cosmochim. Acta*, *62*, 51–68.

Corredor, J. E., and J. M. Morell (2001), Seasonal variation of physical and biogeochemical features in eastern Caribbean surface water, *J. Geophys. Res.*, *106*, 4517–4525.

Deuser, W. G. (1973), Cariaco Trench: Oxidation of organic matter and residence time of anoxic water, *Nature*, *242*, 601–603.

Eglinton, T. I., M. H. Conte, G. Eglinton, and J. M. Hayes (2001), Proceedings of a workshop on alkenones-based paleoceanographic indicators, *Geochem. Geophys. Geosyst.*, *2*, Paper number 2000GC000122. (Available at http://gcubed.magnet.fsu.edu/main.html)

Epstein, B. L., S. D'Hondt, and P. E. Hargraves (2001), The possible metabolic role of C37 alkenones in *Emiliania huxleyi*, *Org. Geochem.*, *32*, 867–875.

Falkowski, P., and D. A. Kiefer (1985), Chlorophyll fluorescence in phytoplankton: Relationship to photosynthesis and biomass, *J. Plankton Res.*, *7*, 715–731.

Goni, M., M. Yunker, R. Macdonald, and E. Ti (2000), Distribution and sources of organic biomarkers in arctic sediments from the Mackenzie River and Beaufort Shelf, *Mar. Chem.*, *71*, 23–51.

Goni, M. A., D. M. Hartz, R. C. Thunell, and E. Tappa (2001), Oceanographic considerations for the application of the alkenone-based paleotemperature UK′37 index in the Gulf of California, *Geochim. Cosmochim. Acta*, *65*, 545–557.

Goni, M. A., H. L. Aceves, R. C. Thunell, E. Tappa, D. Black, Y. Astor, R. Varela, and F. Müller-Karger (2003), Biogenic fluxes in the Cariaco Basin: A combined study of sinking particulates and underlying sediments, *Deep Sea Res., Part I*, *50*, 781–807.

Grimalt, J. O., J. Rullkotter, M.-A. Sicre, R. Summons, J. Farrington, H. R. Harvey, M. Goñi, and K. Sawada (2000), Modification of the C37 alkenone and alkenoate composition in the water column and sediment: Possible implications for sea surface temperature estimates in paleoceanography, *Geochem. Geophys. Geosyst.*, *1*, Paper number 2000GC000053. (Available at http://gcubed.magnet.fsu.edu/main.html)

Harvey, H. R. (2000), Alteration processes of alkenones and related lipids in water columns and sediments, *Geochem. Geophys. Geosyst.*, *1*, Paper number 2000GC000054. (Available at http://gcubed.magnet.fsu.edu/main.html)

Haug, G. H., T. F. Pedersen, D. M. Sigman, S. E. Calvert, B. Nielsen, and L. C. Peterson (1998), Glacial/interglacial variations in production and nitrogen fixation in the Cariaco Basin during the last 580 kyr, *Paleoceanography*, *13*, 427–432.

Haug, G., K. Hughen, D. Sigman, L. Peterson, and U. Rohl (2001), Southward migration of the intertropical convergence zone through the Holocene, *Science*, *293*, 1304–1308.

Henrichs, S. M. (1997), Early diagenesis of organic matter in marine sediments: Progress and perplexity, *Mar. Chem.*, *39*, 119–149.

Herbert, T. D. (2001), Review of alkenones calibrations (culture, water column, and sediments), *Geochem. Geophys. Geosyst.*, *2*, Paper number 2000GC000055. (Available at http://gcubed.magnet.fsu.edu/main.html)

Herbert, T., and J. D. Schuffert (2000), 16 Alkenone unsaturation estimates of sea-surface temperatures at site 1002 over a full glacial cycle, *Proc. Ocean Drill. Program. Sci. Results*, *165*, 239–247.

Herbert, T. D., J. D. Schuffert, and D. Thomas (1998), Depth and seasonality of alkenone production along the California margin inferred from a core top transect, *Paleoceanography*, *13*, 263–271.

Herrera, L. E., and G. Febres-Ortega (1975), Procesos de surgencia y de renovacion de aquas en la Fosa de Cariaco, Mar Caribe, *Bol. Inst. Oceanogr. Univ. Oriente*, *14*, 31–44.

Holm-Hansen, O., C. J. Lorenzen, R. W. Holmes, and J. D. H. Strickland (1965), Fluorometric determination of chlorophyll, *J. Cons. Cons. Int. Explor. Mer.*, *30*, 3–15.

Honjo, S., and K. Doherty (1988), Large-aperture time series oceanic sediment traps: Design objectives, construction and application, *Deep Sea Res.*, *35*, 133–149.

Hughen, K. A., J. T. Overpeck, L. C. Peterson, and R. F. Anderson (1996), The nature of varved sedimentation in the Cariaco Basin, Venezuela, and its paleoclimatic significance, in *Palaeoclimatology and Palaeoceanography From Laminated Sediments*, edited by A. E. S. Kemp, *Geol. Soc. Spec. Publ.*, 116, 171–183.

Hughen, K., J. Southon, S. Lehman, and J. Overpeck (2000), Synchronous radiocarbon and climate shifts during the last deglaciation, *Science*, *290*, 1951–1954.

Jasper, J. P., and J. M. Hayes (1990), A carbon isotopic record of CO_2 levels during the late Quaternary, *Nature*, *347*, 462–464.

Jasper, J. P., J. M. Hayes, A. C. Mix, and F. G. Prahl (1994), Photosynthetic fractionation of ^{13}C and concentrations of dissolved CO_2 in the central equatorial Pacific during the last 255,000 years, *Paleoceanography*, *9*, 781–798.

Lea, D. W., D. K. Pak, L. C. Peterson, and K. A. Hughen (2003), Synchroneity of tropical and high-latitude Atlantic temperatures over the last glacial termination, *Science*, *301*, 1361–1364.

Lidz, L., W. B. Charm, M. M. Ball, and S. Valdes (1969), Marine basins off the coast of Venezuela, *Bull. Mar. Sci.*, *19*, 1–17.

Marlowe, I. T., S. C. Brassell, G. Eglinton, and J. C. Green (1984), Long chain unsaturated ketones and esters in living algae and marine sediments, *Org. Geochem.*, *6*, 135–141.

Mix, A. C., E. Bard, G. Eglinton, L. D. Keigwin, A. C. Ravelo, and Y. Rosenthal (2000), Alkenones and multiproxy strategies in paleoceanographic studies, *Geochem. Geophys. Geosyst.*, *1*, Paper number 2000GC000056. (Available at http://gcubed.magnet.fsu.edu/main.html)

Müller, P. J., and G. Fischer (2001), A 4-year sediment trap record of alkenones from the filamentous upwelling region off Cape Blanc, NW Africa and a comparison with distributions in underlying sediments, *Deep Sea Res., Part I*, *48*, 1877–1903.

Müller, P. J., G. Kirst, G. Ruhland, V. I. Storch, and A. Rosell-Melé (1998), Calibration of the alkenones paleotemperature index UK′37 based on core-tops from the eastern South Atlantic and the global ocean (60°N–60°S), *Geochim. Cosmochim. Acta*, *62*, 1757–1772.

Müller-Karger, F., et al. (2001), Annual cycle of primary production in the Cariaco Basin: Response to upwelling and implications for vertical export, *J. Geophys. Res.*, *106*, 4527–4542.

Overpeck, J., L. Peterson, N. Kipp, and D. Rind (1989), Climate change in the circum-North Atlantic region during the last deglaciation, *Nature*, *338*, 553–557.

Pagani, M., M. A. Arthur, and K. H. Freeman (1999), Miocene evolution of atmospheric carbon dioxide, *Paleoceanography*, *14*, 273–292.

Pelejero, C., and E. Calvo (2003), The upper end of the UK'37 temperature calibration revisited, *Geochem. Geophys. Geosyst.*, *4*, Paper number 2002GC000431. (Available at http://gcubed.magnet.fsu.edu/main.html)

Peterson, L. C., J. T. Overpeck, N. G. Kipp, and J. Imbrie (1991), A high-resolution late quaternary upwelling record from the anoxic Cariaco Basin, Venezuela, *Paleoceanography*, *6*, 99–119.

Popp, B. N., K. L. Hanson, J. E. Dore, R. R. Bidigare, E. A. Laws, and S. G. Wakeham (1999), Controls on the carbon isotopic composition of plankton: Paleoceanographic perspectives, in *Reconstructing Ocean History: A Window into the Future*, edited by A. C. Mix, pp. 381–398, Plenum, New York.

Prahl, F. G., and S. G. Wakeham (1987), Calibration of unsaturation patterns in long-chain ketone compositions for palaeotemperature assessment, *Nature*, *330*, 367–369.

Prahl, F. G., L. A. Muelhausen, and D. A. Zahnle (1988), Further evaluation of long-chain alkenones as indicators of paleoceanographic conditions, *Geochim. Cosmochim. Acta*, *52*, 2303–2310.

Prahl, F. G., R. W. Collier, J. Dymond, M. Lyle, and M. A. Sparrow (1993), A biomarker perspective on prymniesophyte productivity in the northeast Pacific Ocean, *Deep Sea Res., Part I*, *40*, 2061–2076.

Prahl, F. G., J. Dymond, and M. A. Sparrow (2000a), Annual biomarker record for export production in the central Arabian Sea, *Deep Sea Res., Part II*, *47*, 1581–1604.

Prahl, F. G., T. Herbert, S. C. Brassell, N. Ohkouchi, M. Pagani, D. Repeta, A. Rosell-Melé, and E. Sikes (2000b), Status of alkenone paleothermometer calibration: Report from Working Group 3, *Geochem. Geophys. Geosyst.*, *1*, Paper number 2000GC000058. (Available at http://gcubed.magnet.fsu.edu/main.html)

Prahl, F. G., G. V. Wolfe, and M. A. Sparrow (2003), Physiological impacts on alkenone paleothermometry, *Paleoceanography*, *18*, 1025–1032.

Reuer, M. K., E. A. Boyle, and J. E. Cole (2003), A mid-twentieth century reduction in tropical upwelling inferred from coraline trace element proxies, *Earth Planet. Sci. Lett.*, *210*, 437–452.

Richards, F. A. (1975), The Cariaco Basin (Trench), *Oceanogr. Mar. Biol. Annu. Rev.*, *13*, 11–67.

Rosell-Melé, A., J. Carter, A. T. Parry, and G. Eglinton (1995a), Determination of the UK′37 index in geological samples, *Anal. Chem.*, *67*, 1283–1289.

Rosell-Melé, A., G. Eglinton, U. Pflaumann, and M. Sarnthein (1995b), Atlantic core top calibration of the UK′37 index as a sea-surface temperature indicator, *Geochim. Cosmochim. Acta*, *59*, 3099–3107.

Sachs, J. P., R. Schneider, T. I. Eglinton, K. H. Freeman, G. Ganssen, J. F. McManus, and D. W. Oppo (2000), Alkenones as paleoceanographic proxies, *Geochem. Geophys. Geosyst.*, *1*, Paper number 2000GC000059. (Available at http://gcubed.magnet.fsu.edu/main.html)

Scranton, M. I., Y. Astor, R. Bohrer, T.-Y. Ho, and F. E. Müller-Karger (2001), Controls on temporal variability of the geochemistry of the deep Cariaco Basin, *Deep Sea Res., Part I*, *48*, 1605–1625.

Sonzogni, C., E. Bard, F. Rostek, R. Lafont, A. Rosell-Melé, and G. Eglinton (1997), Core-top calibration of the alkenone index versus sea surface temperature in the Indian Ocean, *Deep Sea Res., Part II*, *44*, 1445–1460.

Steinberg, D. K., C. A. Carlson, N. R. Bates, R. J. Johnson, A. F. Michaels, and A. H. Knap (2001), Overview of the US JGOFS Bermuda Atlantic

Time-series Study (BATS): A decade-scale look at ocean biology and biogeochemistry, *Deep Sea Res., Part II*, *48*, 1405–1447.

Sun, M.-Y., and S. G. Wakeham (1994), Molecular evidence for degradation and preservation of organic matter in the anoxic Black Sea Basin, *Geochim. Cosmochim. Acta*, *58*, 3395–3406.

Taylor, G. T., M. Iabichella, T.-Y. Ho, M. I. Scranton, R. C. Thunell, F. Müller-Karger, and R. Varela (2001), Chemoautotrophy in the redox transition zone of the Cariaco Basin: A significant midwater source of organic carbon production, *Limnol. Oceanogr.*, *46*, 148–163.

Thunell, R. C., R. Varela, M. Llano, J. Collister, F. Müller-Karger, and R. Bohrer (2000), Organic carbon fluxes, degradation, and accumulation in an anoxic basin: Sediment trap results from the Cariaco Basin, *Limnol. Oceanogr.*, *45*, 300–308.

Villanueva, J., J. O. Grimalt, L. D. Labeyrie, E. Cortijo, L. Vidal, and J.-L. Turon (1998), Precessional forcing of productivity in the North Atlantic Ocean, *Paleoceanography*, *13*, 561–571.

Volkman, J. K. (2000), Ecological and environmental factors affecting alkenones distributions in seawater and sediments, *Geochem. Geophys. Geosyst.*, *1*, Paper number 2000GC000061. (Available at http://gcubed.magnet.fsu.edu/main.html)

Volkman, J. K., G. Eglinton, E. D. S. Corner, and T. E. V. Forsberg (1980), Long-chain alkenes and alkenones in the marine coccolithophorids *Emiliania huxleyi*, *Phytochemistry*, *19*, 2619–2622.

Volkman, J. K., S. M. Barrett, S. I. Blackburn, and E. L. Sikes (1995), Alkenones in Gephyrocapsa oceanica: Implications for studies of paleoclimate, *Geochim. Cosmochim. Acta*, *59*, 513–520.

Walsh, J. J., et al. (1999), Simulation of carbon-nitrogen cycling during spring upwelling in the Cariaco Basin, *J. Geophys. Res.*, *104*, 7807–7825.

Weaver, P. P. E., M. R. Chapman, G. Eglinton, M. Zhao, D. Rutledge, and G. Read (1999), Combined coccolith, foraminiferal, and biomarker reconstruction of paleoceanographic conditions over the past 120 kyr in the northern North Atlantic (59°N, 23°W), *Paleoceanography*, *14*, 336–349.

Werne, J. P., D. J. Hollander, T. W. Lyons, and L. C. Peterson (2000), Climate-induced variations in productivity and planktonic ecosystem structure from the Younger Dryas to Holocene in the Cariaco Basin, Venezuela, *Paleoceanography*, *15*, 19–29.

Westrich, J. T., and R. A. Berner (1984), The role of sedimentary organic matter in bacterial sulfate reduction: The G model tested, *Limnol. Oceanogr.*, *29*(2), 236–249.

Winter, A., B. Rost, H. Hilbrecht, and M. Elbrachter (2002), Vertical and horizontal distribution of coccolithophores in the Caribbean Sea, *Geo Mar. Lett.*, *22*, 150–161.

Yarincik, K. M., R. W. Murray, T. W. Lyons, L. C. Peterson, and G. H. Haug (2000), Oxygenation history of bottom waters in the Cariaco Basin, Venezuela, over the past 578,000 years: Results from redox-sensitive metals (Mo, V, Mn, and Fe), *Paleoceanography*, *15*, 593–604.

H. L. Aceves, M. A. Goni, E. Tappa, R. C. Thunell, and M. P. Woodworth, Department of Geological Sciences, University of South Carolina, Columbia, SC 29208, USA. (goni@geol.sc.edu; tappa@geol.sc.edu; thunell@geol.sc.edu; mwoodworth@geol.sc.edu)

Y. Astor and R. Varela, Estacion de Investigaciones Marinas de Margarita, Fundacion La Salle de Ciencias Naturales, Aptdo. 144, Porlamar 6301, Venezuela. (yastor@edimar.org; rvarela@edimar.org)

D. Black, Department of Geology, 252 Buchtel Common, University of Akron, Akron, OH 44325-4101, USA. (dblack1@uakron.edu)

F. Müller-Karger, Department of Marine Science, University of South Florida, St. Petersburg, FL 33701, USA. (carib@seas.marine.usf.edu)